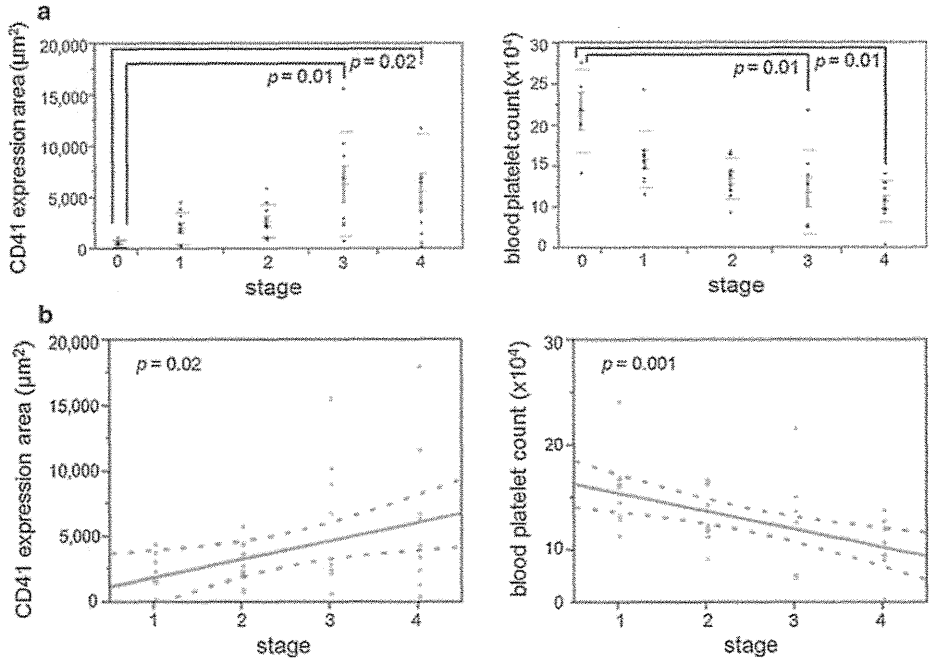

Fig. 1 Relationship between histological liver damage and either the CD41 expression area in the noncancerous liver tissues or the blood platelet count. **a** The noncancerous liver tissues with cirrhosis had a larger CD41 expression area than seen in the controls ($p = 0.02$, $p < 0.05$), although the blood platelet count was small. **b** In the noncancerous liver tissues with chronic hepatitis and cirrhosis, the CD41 expression area increased with increasing histological liver damage ($p = 0.02$, $p < 0.05$), although the blood platelet count decreased ($p = 0.001$, $p < 0.05$)

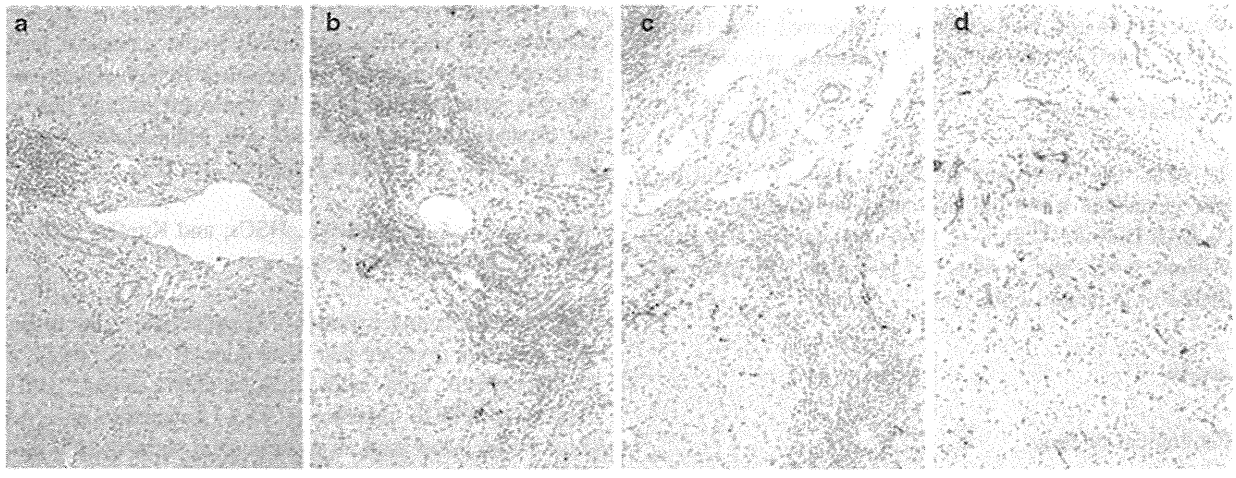

Fig. 2 Typical immunostaining for CD41 in a periportal area of noncancerous liver tissues with chronic hepatitis or cirrhosis. In noncancerous liver tissues with chronic hepatitis or cirrhosis, CD41-positive reactions are present predominantly in the sinusoidal space of the periportal area with inflammation. In high-stage cases, strong CD41 positive reactions are observed along the destroyed limiting plate of the expanded fibrous portal area with inflammation, and in the sinusoidal space of the periportal area. Labeled streptavidin biotin with CD41 antibody: **a** grade 1, stage 1; **b** grade 2, stage 2; **c** grade 2, stage 3; **d** grade 2, stage 4

When the platelet and Kupffer cell areas in the cancerous and non-cancerous tissues were compared, the platelet and Kupffer cell areas were significantly smaller in cancerous tissue than in noncancerous tissue (Fig. 4a, platelet area: 492 ± 823 vs. 3643 ± 4055 μm^2, $p = 0.001$, $p < 0.05$; Fig. 4b, Kupffer cell area: 450 ± 841 vs. 3012 ± 3051 μm^2, $p = 0.001$, $p < 0.05$). Regardless of the liver damage in noncancerous tissue, both the platelet and Kupffer cell areas in cancerous tissue were smaller than those in noncancerous tissue. The platelet and Kupffer cell areas in cancerous tissue tended to decrease with decreasing histological differentiation of HCC (Table 2). We also measured with regard to the

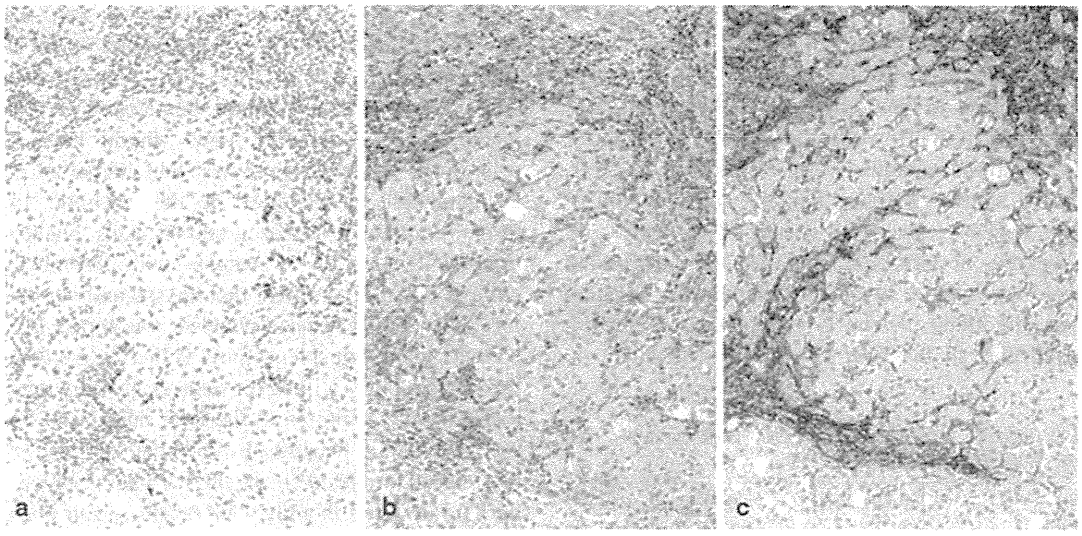

Fig. 3 Typical immunostaining for CD41, PDGF receptor-β, and smooth muscle actin in the periportal area of noncancerous liver tissues with cirrhosis. **a** Platelets are present in the periportal area with inflammation. Labeled streptavidin biotin with CD41 antibody. **b** Serial section shown in **a** stained for PDGF receptor-β antibody. Portal mesenchymal and perisinusoidal cells are stained for PDGF receptor-β. These are dense in the periportal area, where platelets are frequently observed in **a**. Labeled streptavidin biotin with PDGF receptor-β antibody. **c** Serial section shown in **b** stained with smooth muscle actin. Most of the stained cells are identical to those stained for PDGF receptor-β in **b**. Labeled streptavidin biotin with smooth muscle actin antibody

Kupffer cell count. The results evaluated by Kupffer cell count correlate with those evaluated by Kupffer cell areas. The Kupffer cell count was significantly smaller in cancerous tissue than in noncancerous tissue (data was not shown).

Electron microscopic findings

In the sinusoidal space of noncancerous tissues with cirrhosis, there were platelets with dense granules and α-granules. They were partly attached to the sinusoidal endothelial cells (Fig. 5a). Some of the platelets had several empty granules, which are indicative of degranulation (Fig. 5b). Platelets were rarely found in the space of Disse. Around platelets that adhered to the sinusoidal endothelial cells, HSCs that were more spindle-shaped and had a few fat droplets were observed (Fig. 5c). Platelets were not in direct contact with HSCs and Kupffer cells.

Discussion

Blood platelets, by connecting hemostasis and inflammatory processes, participate in the pathogenesis of chronic liver disease. In this study, we demonstrated the pathological findings for the accumulation of platelets in the liver in cases with chronic hepatitis C.

Hill-Zobel et al. [32] studied platelet dynamics in healthy humans using ^{111}In-labeled platelets. They reported

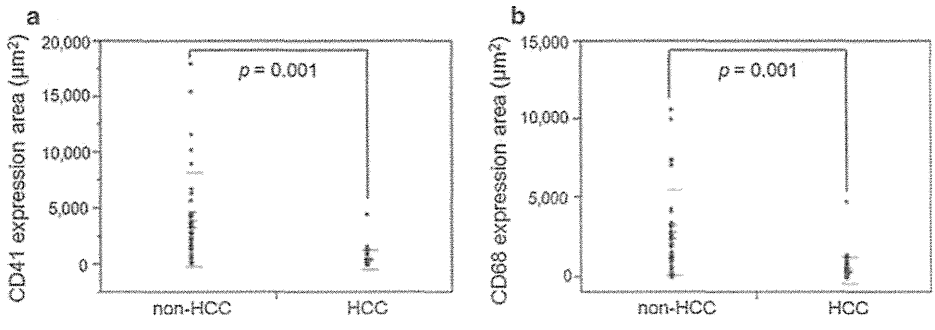

Fig. 4 CD41 (**a**) and CD68 (**b**) expression areas in different tissue types (HCC vs. non-HCC). Both the platelet and Kupffer cell areas are significantly smaller in HCC tissue than those in nonHCC tissue (platelet area: 492 ± 823 vs. 3643 ± 4055 μm^2, $p = 0.001$, $p < 0.05$; Kupffer cell area: 450 ± 841 vs. 3012 ± 3051 μm^2, $p = 0.001$, $p < 0.05$)

that the uptake in the liver was 12.6 % at 30 min and 24 % at ten days, and that in the spleen was 42.7 % at 30 min and 37 % at ten days in healthy humans [32]. The accumulation of platelets in the normal control liver tissue was confirmed in this study. However, the platelet dynamics of patients with chronic hepatitis or cirrhosis are not yet clear. In the current study, we found that the accumulation of platelets in noncancerous liver tissues of patients with chronic hepatitis or cirrhosis increased with increasing histological liver damage. In patients with chronic hepatitis or cirrhosis, the blood platelet level gradually decreased, and was reflected in the liver damage. As there are no megakaryocytes in liver tissues, we can distinguish between platelets that have accumulated in the sinusoidal space and are derived from bone marrow from those derived from extramedullary hematopoiesis. The extramedullary hematopoietic tissue should have hematinic cells, such as megakaryocytes, and immature cells. The accumulation of platelets in the cirrhotic liver with thrombocytopenia has been shown using platelet scintigraphy [17, 23–25]. In patients with thrombocytopenia, Kinuya et al. [24] reported that the spleen/liver uptake ratio for ^{111}In- or ^{99}Tc-labeled platelets was apparently lower in patients for whom splenectomy is ineffective than in those for whom it was effective. Sata et al. [25] reported that platelets were captured in the liver during interferon therapy for chronic hepatitis B, and that this phenomenon is one cause of the decrease in peripheral blood platelets during interferon therapy. The results of our present study are not necessarily contrary to the established theory of thrombocytopenia with chronic hepatitis. It has been reported that the mechanisms leading to thrombocytopenia in cirrhosis most likely involve multifactorial processes [17–22]. We consider that the accumulation of platelets in the liver with chronic hepatitis and cirrhosis may be one of the important contributory factors to thrombocytopenia.

Table 2 Relationship between histological differentiation and platelet area or Kupffer cell area in HCCs

Histological differentiation	Platelet area (μm^2)	Kupffer cell area (μm^2)
Well ($n = 2$)[a]	1532 ± 26	2674 ± 3094
Moderate ($n = 35$)[a]	440 ± 82	305 ± 405
Poor ($n = 1$)	225	108

well well differentiated HCC, *moderate* moderately differentiated HCC, *poor* poorly differentiated HCC

[a] Mean ± SD

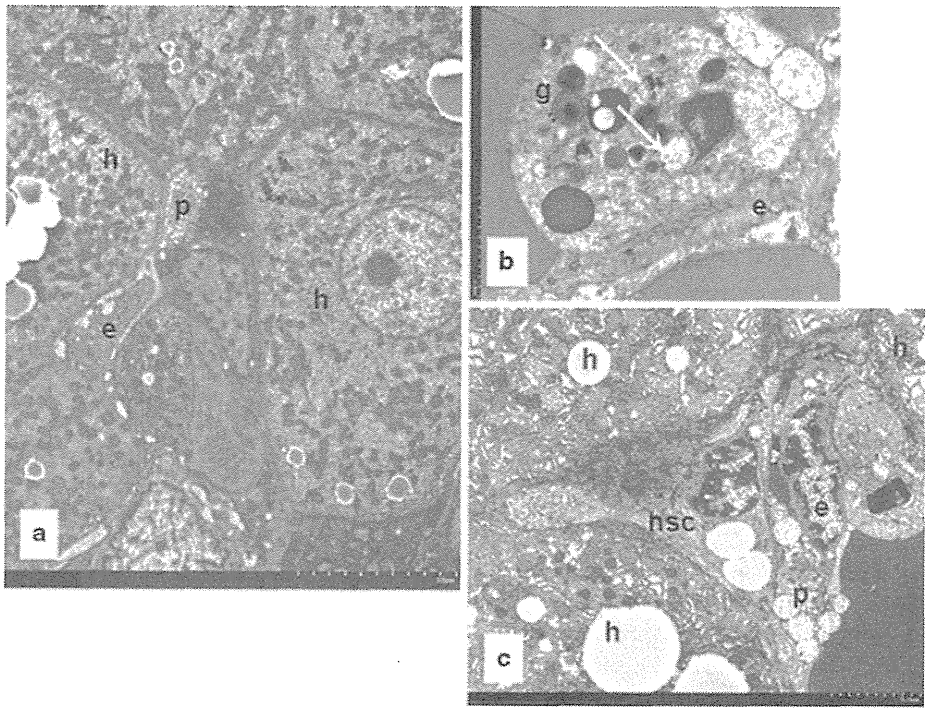

Fig. 5 Electron micrographs of a cirrhotic liver. **a** Platelets (*p*) in the sinusoidal space adhere to endothelial cells (*e*). **b** A platelet that has adhered to a sinusoidal endothelial cell contains both α-granules (*g*) and empty ones (*arrows*). **c** Around platelets that have adhered to a sinusoidal endothelial cell, a hepatic stellate cell (*hsc*)—which is more spindle-shaped, and has a few fat droplets—can be observed. *h* hepatocytes; **a** ×5000, **b** ×25000; **c** ×7000

Histologically, platelets in noncancerous liver tissues of patients with chronic hepatitis or cirrhosis are seen predominantly in the sinusoidal space of the periportal area with inflammation. As viewed through an electron microscope, the platelets aggregate in the sinusoids and adhere to the sinusoidal endothelial cells. Platelets contain four types of distinguishable granules or vesicles: dense granules, lysosomes, peroxisomes, and α-granules. These granules contain various active compounds. Blood platelets, activated in inflammatory and immune processes, release different intraplatelet compounds [1]. Platelets transport these active compounds in their granules to the target cells [2, 3]. Platelets then adhere to endothelial cells or exposed subendothelial matrices. Following adhesion, they become activated and secrete granule content. The accumulation of platelets in the liver and the adhesion to the sinusoidal endothelial cells are important steps in direct platelet action for the liver. In blood vessels, the vessel wall, with its inner lining of endothelium, is crucial to the maintenance of a patent vasculature. The endothelium contains thromboregulators—nitric oxide, prostacyclin, and the ectonucleotidase CD39—which together provide a defence against platelet thrombus formation [33]. When the endothelium is disrupted, collagen and tissue factor become exposed to the flowing blood, thereby initiating the formation of thrombus. Endothelium is also an important target for tumor necrosis factor (TNF) and interleukin-1 (IL-1). The endothelium synthesizes and releases platelet activating factor (PAF) in response to TNF. This activity of TNF overlaps that of IL-1, which also induces PAF production in endothelium [34]. These vessel wall alterations result in a change in endothelium from antithrombotic to thrombotic. The disrupted endothelium is the first reaction in platelet adhesion to the vessel subendothelium under physiologic blood flow [33]. In the presence of TNF-α-induced sinusoidal alteration, platelets adhere to sinusoidal endothelial cells in the same way as to vessel walls [35]. Characteristic pathological features of chronic HCV infection are chronic inflammation and apoptosis of infected and bystander hepatocytes [36, 37]. In a model of hepatitis, Kupffer cells produced the majority of TNF-α [38]. Under lipopolysaccharide administration in mice, TNF or IL-1 induce platelets to accumulate in the liver sinusoidal space within a few minutes by a different mechanism of aggregation [39–41]. With the depletion of Kupffer cells, platelets do not accumulate in the liver after lipopolysaccharide administration [41]. Kupffer cells are involved in various mechanisms, such as phagocytosis, metabolism, cytokine generation, and antitumor effect. Platelets may accumulate in the sinusoidal space under thrombocytotic conditions in chronic hepatitis C brought about by the activated hepatic reticuloendothelial system, as caused by inflammation through the mechanism involving the activation of Kupffer cells.

The role of platelets in the pathogenesis of chronic hepatitis and cirrhosis is not clear. We suggest that platelet-derived factor and liver condition should be taken into account when examining the role of platelets in the liver. We identified a dense population of cells expressing PDGF receptor-β in the periportal areas of cirrhotic liver, whereas only a few mesenchymal cells stained for this peptide were seen in patients at the lower stage of chronic hepatitis and in controls. In addition, most of the PDGF receptor-β expressing cells were also stained for smooth muscle actin. These cells, which play a central role in liver fibrosis, are believed to be transformed from HSCs [29–31], and their proliferation is stimulated by PDGF [42]. HSCs are increasingly being seen as key mediators in the progression of liver fibrosis. In this study, HSCs expressing PDGF receptor-β were located in the periportal area, where platelets were frequently observed. PDGF is the basic mediator involved in platelet granules. PDGF overexpression has been linked to different types of fibrotic disorders and malignancies [43]. In chronic liver disease, the essential role of all PDGF family members in liver fibrosis has been demonstrated [42, 44–47]. To date, four members of the PDGF family have been identified: PDGF-A, PDGF-B, PDGF-C, and PDGF-D [48]. PDGF-B has a stimulating influence on the fibrogenesis and mitogenesis of HSCs in the liver [42]. The biological effects of PDGF are elicited through binding to two specific receptors, PDGF receptor-α and PDGF receptor-β. The binding affinity of PDGF receptor-β is restricted to PDGF-B [49]. When HSCs expressing PDGF receptor-β are present in the liver, the liver may be susceptible to PDGF contained in platelets. The accumulation of platelets in the liver with chronic hepatitis may be involved in liver fibrosis through the activated HSCs.

We also found that the platelet area was significantly smaller in cancerous tissue than that in noncancerous tissues. It has been reported that the number of Kupffer cells in cancerous tissues decreased in comparison with the number in noncancerous tissues as the histological differentiation of HCC decreased [50]. Indeed, the Kupffer cell area in cancerous tissues was significantly smaller than that in noncancerous tissues and tended to decrease with decreasing histological differentiation of HCC in this study. We consider that platelets may also accumulate in the blood space in cancerous tissue through some mechanisms involving the Kupffer cells.

In conclusion, the results obtained in the present study indicate that the accumulation of platelets in the liver with chronic hepatitis C may be involved in thrombocytopenia and liver fibrosis through the activated HSCs. In addition, platelets may accumulate in the sinusoidal space through another mechanism involving the activation of Kupffer cells. Further study of the biological characteristics and

function of these cells will contribute to improving the treatment of thrombocytopenia and liver fibrosis.

Conflict of interest The authors declare that they have no conflict of interest.

References

1. Mannaioni PF, Di Bello MG, Masini E. Platelets and inflammation: role of platelet-derived growth factor, adhesion molecules and histamine. Inflamm Res. 1997;46:4–18.
2. Handagama PJ, George JN, Shuman MA, McEver RP, Bainton DF. Incorporation of a circulating protein into megakaryocyte and platelet granules. Proc Natl Acad Sci USA. 1987;84:861–5.
3. Verheul HMW, Hoekman K, Bakker SL, Eekman CA, Folman CC, Broxterman HJ, et al. Platelet: transporter of vascular endothelial growth factor. Clin Cancer Res. 1997;3:2187–90.
4. Italiano JE Jr, Richardson JL, Patel-Hett S, Battinelli E, Zaslavsky A, Short S, et al. Angiogenesis is regulated by a novel mechanism: pro- and antiangiogenic proteins are organized into separate platelet α granules and differentially released. Blood. 2008;111:1227–33.
5. Brill A, Dashevsky O, Rivo J, Gozal Y, Varon D. Platelet-derived microparticles induce angiogenesis and stimulate post-ischemic revascularization. Cardiovasc Res. 2005;67:30–8.
6. Janowska-Wieczorek A, Wysoczynski M, Kijowski J, Marquez-Curtis L, Machalinski B, Ratajczak J, et al. Microvesicles derived from activated platelets induce metastasis and angiogenesis in lung cancer. Int J Cancer. 2005;113:752–60.
7. Gilsanz F, Escalante F, Auray C, Olbes AG. Treatment of leg ulcers in β-thalassaemia intermedia: use of platelet-derived wound healing factors from the patient's own platelets. Br J Haematol. 2001;115:710.
8. Mazzucco L, Medici D, Serra M, Panizza R, Rivara G, Orecchia S, et al. The use of autologous platelet gel to treat difficult-to-heal wounds: a pilot study. Transfusion. 2004;44:1013–8.
9. Lesurtel M, Graf R, Aleil B, Walther DJ, Tian Y, Jochum W, et al. Platelet-derived serotonin mediates liver regeneration. Science. 2006;312:104–7.
10. Nash GF, Turner LF, Scully MF, Kakkar AK. Platelets and cancer. Lancet Oncol. 2002;3:425–30.
11. Camerer E, Qazi AA, Duong DN, Cornelissen I, Advincula R, Coughlin SR. Platelets, protease-activated receptors, and fibrinogen in hematogenous metastasis. Blood. 2004;104:397–401.
12. Iannacone M, Sitia G, Isogawa M, Marchese P, Castro MG, Lowenstein PR, et al. Platelets mediate cytotoxic T lymphocyte-induced liver damage. Nat Med. 2005;11:1167–9.
13. Lang PA, Contaldo C, Georgiev P, El-Badry AM, Recher M, Kurrer M, et al. Aggravation of viral hepatitis by platelet-derived serotonin. Nat Med. 2008;14:756–61.
14. Bataller R, Brenner DA. Liver fibrosis. J Clin Invest. 2005; 115:209–18.
15. Friedman SL. Liver fibrosis-from bench to bedside. J Hepatol. 2003;38(Suppl 1):S38–53.
16. Witters P, Freson K, Verslype C, Peerlinck K, Hoylaerts M, Nevens F, et al. Review article: blood platelet number and function in chronic liver disease and cirrhosis. Aliment Pharmacol Ther. 2008;27:1017–29.
17. Aoki Y, Hirai K, Tanikawa K. Mechanism of thrombocytopenia in liver cirrhosis: kinetics of indium-111 tropolone labelled platelets. Eur J Nucl Med. 1993;20:123–9.
18. Schmidt KG, Rasmussen JW, Bekker C, Madsen PE. Kinetics and in vivo distribution of 111-In-labelled autologous platelets in chronic hepatic disease: mechanisms of thrombocytopenia. Scand J Haematol. 1985;34:39–46.
19. Toghill PJ, Green S. Splenic influences on the blood in chronic liver disease. Q J Med. 1979;48:613–25.
20. Aster RH. Pooling of platelets in the spleen: role in the pathogenesis of "hypersplenic" thrombocytopenia. J Clin Invest. 1966; 45:645–57.
21. Peck-Radosavljevic M. Thrombocytopenia in liver disease. Can J Gastroenterol. 2000;14:60D–6D.
22. Kajihara M, Okazaki Y, Kato S, Ishii H, Kawakami Y, Ikeda Y, et al. Evaluation of platelet kinetics in patients with liver cirrhosis: similarity to idiopathic thrombocytopenic purpura. J Gastroenterol Hepatol. 2007;22:112–8.
23. Noguchi H, Hirai K, Aoki Y, Sakata K, Tanikawa K. Changes in platelet kinetics after a partial splenic arterial embolization in cirrhotic patients with hypersplenism. Hepatology. 1995;22: 1682–8.
24. Kinuya K, Matano S, Nakashima H, Taki S. Scintigraphic prediction of therapeutic outcomes of splenectomy in patients with thrombocytopenia. Ann Nucl Med. 2003;17:161–4.
25. Sata M, Yano Y, Yoshiyama Y, Ide T, Kumashiro R, Suzuki H, et al. Mechanism of thrombocytopenia induced by interferon therapy for chronic hepatitis B. J Gastroenterol. 1997;32: 206–10.
26. Desmet VJ, Gerber M, Hoofnagle JH, Manns M, Scheuer PJ. Classification of chronic hepatitis: diagnosis, grading and staging. Hepatology. 1994;19:1513–20.
27. Batts KP, Ludwig J. Chronic hepatitis. An update on terminology and reporting. Am J Surg Pathol. 1995;19:1409–17.
28. Hirohashi S, Blum HE, Ishak KG, Deugnier Y, Kojiro M, Laurent Puig P, et al. Tumours of the liver and intrahepatic bile ducts. Hepatocellular carcinoma. In: Hamilton SR, Aaltonen LA, editors. Pathology and genetics of tumor of the digestive system. World Health Organization Classification of Tumors. Lyon: IARC Press; 2000. p. 159–72.
29. Pinzani M, Milani S, Herbst H, DeFranco R, Grappone C, Gentilini A, et al. Expression of platelet-derived growth factor and its receptors in normal human liver and during active hepatic fibrogenesis. Am J Pathol. 1996;148:785–800.
30. Blomhoff R, Wake K. Perisinusoidal stellate cells of the liver: important roles in retinol metabolism and fibrosis. FASEB J. 1991;5:271–7.
31. Ikura Y, Morimoto H, Ogami M, Jomura H, Ikeoka N, Sakurai M. Expression of platelet-derived growth factor and its receptor in livers of patients with chronic liver disease. J Gastroenterol. 1997;32:496–501.
32. Hill-Zobel RL, McCandless B, Kang SA, Chikkappa G, Tsan MF. Organ distribution and fate of human platelets: studies of asplenic and splenomegalic patients. Am J Hematol. 1986;23:231–8.
33. Furie B, Furie BC. Mechanisms of thrombus formation. N Engl J Med. 2008;359:938–49.
34. Bussolino F, Camussi G, Baglioni C. Synthesis and release of platelet-activating factor by human vascular endothelial cells treated with tumor necrosis factor or interleukin 1α. J Biol Chem. 1988;263:11856–61.
35. Miyazawa Y, Tsutsui H, Mizuhara H, Fujiwara H, Kaneda K. Involvement of intrasinusoidal hemostasis in the development of concanavalin A-induced hepatic injury in mice. Hepatology. 1998;27:497–506.
36. Rehermann B, Nascimbeni M. Immunology of hepatitis B virus and hepatitis C virus infection. Nat Rev Immunol. 2005;5: 215–29.
37. Spengler U, Nattermann J. Immunopathogenesis in hepatitis C virus cirrhosis. Clin Sci. 2007;112:141–55.
38. Dolganiuc A, Norkina O, Kodys K, Catalano D, Bakis G, Marshall C, et al. Viral and host factors induce macrophage activation and loss of toll-like receptor tolerance in chronic HCV infection. Gastroenterology. 2007;133:1627–36.

39. Pearson JM, Schultze AE, Jean PA, Roth RA. Platelet participation in liver injury from Gram-negative bacterial lipopolysaccharide in the rat. Shock. 1995;4:178–86.
40. Itoh H, Cicala C, Douglas GJ, Page CP. Platelet accumulation induced by bacterial endotoxin in rats. Thromb Res. 1996; 83:405–19.
41. Nakamura M, Shibazaki M, Nitta Y, Endo Y. Translocation of platelets into Disse spaces and their entry into hepatocytes in response to lipopolysaccharides, interleukin-1 and tumour necrosis factor: the role of Kupffer cells. J Hepatol. 1998;28: 991–9.
42. Pinzani M, Gesualdo L, Sabbah GM, Abboud HE. Effects of platelet-derived growth factor and other polypeptide mitogens on DNA synthesis and growth of cultured rat liver fat-storing cells. J Clin Invest. 1989;84:1786–93.
43. Dirks RP, Bloemers HP. Signals controlling the expression of PDGF. Mol Biol Rep. 1996;22:1–24.
44. Borkham-Kamphorst E, van Roeyen CRC, Ostendorf T, Floege J, Gressner AM, Weiskirchen R. Pro-fibrogenic potential of PDGF-D in liver fibrosis. J Hepatol. 2007;46:1064–74.
45. Czochra P, Klopcic B, Meyer E, Herkel J, Garcia-Lazaro JF, Thieringer F, et al. Liver fibrosis induced by hepatic overexpression of PDGF-B in transgenic mice. J Hepatol. 2006;45: 419–28.
46. Friedman SL. Mechanisms of hepatic fibrogenesis. Gastroenterology. 2008;134:1655–69.
47. Maass T, Thieringer FR, Mann A, Longerich T, Schirmacher P, Strand D, et al. Liver specific overexpression of platelet-derived growth factor-B accelerates liver cancer development in chemically induced liver carcinogenesis. Int J Cancer. 2011;128:1259–68.
48. Li X, Eriksson U. Novel PDGF family members: PDGF-C and PDGF-D. Cytokine Growth Factor Rev. 2003;14:91–8.
49. Kelly JD, Haldeman BA, Grant FJ, Murray MJ, Seifert RA, Bowen-Pope DF, et al. Platelet-derived growth factor (PDGF) stimulates PDGF receptor subunit dimerization and intersubunit trans-phosphorylation. J Biol Chem. 1991;266:8987–92.
50. Tanaka M, Nakashima O, Wada Y, Kage M, Kojiro M. Pathomorphological study of Kupffer cells in hepatocellular carcinoma and hyperplastic nodular lesions in the liver. Hepatology. 1996; 24:807–12.

Cancer Science
The official journal of the Japanese Cancer Association

Interaction of endothelial progenitor cells expressing cytosine deaminase in tumor tissues and 5-fluorocytosine administration suppresses growth of 5-fluorouracil-sensitive liver cancer in mice

Takuji Torimura,[1,4,5] Takato Ueno,[1] Eitaro Taniguchi,[1] Hiroshi Masuda,[1] Hideki Iwamoto,[1] Toru Nakamura,[1] Kinya Inoue,[1] Osamu Hashimoto,[1] Mitsuhiko Abe,[1] Hironori Koga,[1] Vincenza Barresi,[2] Emi Nakashima,[3] Hirohisa Yano[4] and Michio Sata[1]

[1]Liver Cancer Division, Research Center for Innovative Cancer Therapy and Division of Gastroenterology, Department of Medicine, Kurume University School of Medicine, Kurume, Japan; [2]Department of Chemical Sciences, Section of Biochemistry and Molecular Biology, University of Catania, Catania, Italy; [3]Faculty of Pharmacy, Keio University, Tokyo; [4]Department of Pathology, Kurume University School of Medicine, Kurume, Japan

(Received September 5, 2011/Revised December 2, 2011/Accepted December 5, 2011/Accepted manuscript online December 8, 2011/Article first published online January 25, 2012)

The drug delivery system to tumors is a critical factor in upregulating the effect of anticancer drugs and reducing adverse events. Recent studies indicated selective migration of bone marrow-derived endothelial progenitor cells (EPC) into tumor tissues. Cytosine deaminase (CD) transforms nontoxic 5-fluorocytosine (5-FC) into the highly toxic 5-fluorouracil (5-FU). We investigated the antitumor effect of a new CD/5-FC system with CD cDNA transfected EPC for hepatocellular carcinoma (HCC) in mice. We used human hepatoma cell lines (HuH-7, HLF, HAK1-B, KYN-2, KIM-1) and a rat EPC cell line (TR-BME-2). *Escherichia coli* CD cDNA was transfected into TR-BME-2 (CD-TR-BME). The inhibitory effect of 5-FU on the proliferation of hepatoma cell lines and the inhibitory effect of 5-FU secreted by CD-TR-BME and 5-FC on the proliferation of co-cultured hepatoma cells were evaluated by a tetrazolium-based assay. In mouse subcutaneous xenograft models of KYN-2 and HuH-7, CD-TR-BME was transplanted intravenously followed by 5-FC injection intraperitoneally. HuH-7 cells were the most sensitive to 5-FU and KYN-2 cells were the most resistant. CD-TR-BME secreted 5-FU and inhibited HuH-7 proliferation in a 5-FC dose-dependent manner. CD-TR-BME were recruited into the tumor tissues and some were incorporated into tumor vessels. Tumor growth of HuH-7 was significantly suppressed during 5-FC administration. No bodyweight loss, ALT abnormality or bone marrow suppression was observed. These findings suggest that our new CD/5-FC system with CD cDNA transfected EPC could be an effective and safe treatment for suppression of 5-FU-sensitive HCC growth. (*Cancer Sci* 2012; 103: 542–548)

In 1997, putative endothelial progenitor cells (EPC) were isolated from peripheral blood and shown to be incorporated into the vasculature in adults.[1] The EPC in adults originate from the bone marrow and selectively home to sites with ongoing vascular formation.[2,3]

Vascular development is essential for the growth of solid tumors.[4,5] Accumulating evidence suggests that circulating bone marrow-derived cells, including EPC, migrate into tumor-associated stroma to support vascular formation and tumor development.[6,7] Stromal-derived factor-1 (SDF-1) mainly recruits bone marrow-derived cells to tumor tissues from the peripheral circulation.[8]

Cytosine deaminase (CD) in bacteria and fungi are known to deaminate 5-fluorocytosine (5-FC) to the highly toxic 5-fluorouracil (5-FU).[9,10] Normal mammalian cells do not have CD and are relatively resistant to 5-FC. Gene transfer of *Escherichia coli* CD to mammalian cells renders these cells selectively sensitive to the toxic effects of 5-FC. In many reports of cancer gene therapy with this suicide gene/prodrug system, the most interesting property is the "bystander effect", the death of unmodified tumor cells by 5-FU secretion from CD cDNA transfected cells.[11] Most of these reports have demonstrated the efficacy of the suicide gene/prodrug system.

Hepatocellular carcinoma (HCC) is one of the most common malignant tumors in the tropics and Far East, including Japan.[12] Hepatocellular carcinoma develops multifocally in the cirrhotic liver. Hepatocellular carcinoma is a highly angiogenic tumor, ultimately supplied with neoarteries in parallel with tumor development.[13,14] For advanced non-resectable HCC, chemotherapy with 5-FU is sometimes selected.[15,16] However, the therapeutic efficacy of 5-FU is not fully satisfactory due to liver dysfunction, leukocytopenia and thrombocytopenia caused by the associated liver cirrhosis. To improve the outcome of chemotherapy with 5-FU, it seems important to establish a new drug delivery system to supply a sufficient amount of 5-FU to HCC tissue only without severe adverse effects.

In the present study, we injected rat-derived endothelial progenitor cells, which were transfected with *E. coli* CD cDNA, and administered 5-FC to tumor-bearing mice to evaluate the antitumor effect of the new CD/5-FC system for HCC.

Materials and Methods

Reagents, cells and animals. HUVEC and human hepatoma cell lines (HuH-7, HLF) were obtained from CAMBREX Bio Science Walkersville Inc. (Walkersville, MD, USA). Human hepatoma cell lines (KYN-2, KIM-1, HAK1-B) were provided from the Department of Pathology, Kurume University School of Medicine (Kurume, Japan). TR-BME-2 cells, a cell line derived from rat bone marrow EPC were provided by the Department of Pharmaceutics, Keio University (Tokyo, Japan).[17] Male 5-week-old nude mice (BALB/c nu/nu, Kyudou KK, Fukuoka, Japan) were acclimatized and placed in separate cages. All animals received humane care according to the criteria outlined in the *Guide for the Care and Use of Laboratory Animals* prepared by the National Academy of Sciences and published by the National Institute of Health.[18] The experimental protocol was approved by the Laboratory Animal Care and Use Committee of Kurume University.

Plasmid construction and *in vitro* transfection. A retroviral vector, containing the entire coding sequence of the *E. coli* CD

[5]To whom correspondence should be addressed.
E-mail: tori@med.kurume-u.ac.jp

doi: 10.1111/j.1349-7006.2011.02182.x

gene (pLXSP-CD), was provided by D. F. Condorelli (Department of Chemical Science, Section of Biochemistry and Molecular Biology, University of Catania, Catania, Italy). Transfection of plasmid was performed according to the report by Barresi *et al.*[19]

***In vitro* inhibition of cell proliferation by addition of 5-FU.** Approximately 1000 HUVEC and TR-BME-2 cells transfected with CD cDNA (CD-TR-BME) were added with EGM-2 (Clonetics, San Diego, CA, USA) supplemented with 5% FBS to 96-well plates coated with human fibronectin (Gibco Invitrogen Co., Grand Island, NY, USA) and type 1 collagen (Gibco Invitrogen Co.). Then, 1×10^3 HuH-7, HLF, KIM-1, KYN-2 and HAK1-B in DMEM (Gibco Invitrogen Co.) supplemented with 10% FBS were added. HUVEC, CD-TR-BME cells and human hepatoma cells were incubated at 37°C. After 24 h, 5-FU at 0, 5, 10, 50, 100, 500 or 1000 ng/mL was added to the medium and incubated for 72 h. The cytotoxicity was then evaluated by a tetrazolium-based assay (Cell Count Reagent SF; Nakalai Tesque Inc., Kyoto, Japan).

5-Fluorouracil production by CD-TR-BME cells after the addition of 5-FC. Next, 5×10^4 CD-TR-BME cells were cultured with 1 mL of EBM-2 supplemented with 5% FBS for 24 h at 37°C. Then, 5-FC at 0, 1, 10, 100 or 1000 μg/mL was added to the medium and incubated for 72 h. The concentration of 5-FU in the media was measured using HPLC.

***In vitro* "bystander effect" experiment.** Next, 5×10^3 hepatoma cells (HuH-7, HuH-7, HLF, KIM-1, KYN-2, HAK1-B) were cultured with DMEM supplemented with 10% FBS for 24 h. After confirming that CD-TR-BME cells could not migrate through a 2-μm pore size filter of Chemotaxicell cell-culture chambers (Kurabo Inc., Osaka, Japan), CD-TR-BME cells (5×10^4) were cultured in the chambers with EBM-2 medium containing 5% FBS for 24 h at 37°C. The chambers with the CD-TR-BME cells were then co-cultured with hepatoma cells with EBM-2 medium containing 5% FBS and 5-FC for 72 h. The cytotoxicity against the hepatoma cells was evaluated by a tetrazolium-based assay.

Protocols of treatment with a combination of CD-TR-BME cells and 5-FC. Male nude mice were injected subcutaneously with 5×10^6 HuH-7 cells or KYN-2 cells. After the tumor volume reached 50 mm^3, the mice were divided at random into three groups: the PBS-treated group; the CD-TR-BME cell-injected group; and the CD-TR-BME cells treated with 5-FC group, respectively. After tumor formation, mice of the CD-TR-BME and CD-TR-BME + 5-FC groups received injections of 100 μL of PBS containing 1×10^6 CD-TR-BME cells via the tail vein for 5 days. Mice of the CD-TR-BME + 5-FC group received an intraperitoneal injection of 500 mg/kg of 5-FC for 10 days. All mice were then bred without any treatment for 7 days. Tumor size was measured by calipers in two dimensions every 3 days. The mice were killed at day 21. Tumor volume was calculated by the following equation: length × width^2 × 0.52.

Total RNA extraction and RT-PCR. For total RNA isolation, CD-TR-BME cells or 100 mg of tumor tissues were extracted with Isogen (Nippon Gene, Tokyo, Japan). cDNA was synthesized using 2 μg total RNA. The 20-μL RT reaction consisted of 5× first strand buffer, 0.5 mM dNTP, 50 nM random primers and 20 U SuperScript III reverse transcriptase (Invitrogen, Carlsbad, CA, USA). The RNA and primers were mixed and denatured by heating at 70°C for 10 min; the reverse transcription reaction mixture was then incubated for 30 min at 50°C, followed by 15 min at 70°C. The resulting cDNA was amplified by PCR with primer pairs specific for CD, SDF-1, CXCR4 and GAPDH (Table 1). The PCR products were resolved in 1.5% agarose gels and visualized by ethidium bromide staining and ultraviolet trans-illumination.

Migration of CD-TR-BME cells to tumor tissue and confocal laser scanning microscopy. The CD-TR-BME cells were labeled with PKH26-red (Sigma Chemical Co., St Louis, MO, USA).

Table 1. Primers used in RT-PCR

Gene	Annealing T (°C)	Primer sequences	PCR products (bp)
CD	54	5′-GGA GGCTAACAATGTCGAAT 3′-ATGTTTGCAACTTGCTGACC	1302
Murine SDF-1	60	5′-GGACGCCAAGGTCGTCGCCGTG 3′-TTGCATCTCCCACCCATGTCAG	335
Rat CXCR4	54	5′-ATGGGTTGGTAATCCTGGTC 3′-AGAGTAGGACCGGAAGTAGT	224
GAPDH	60	5′-ACCACAGTCCATGCCATCAC 3′-ATGTCGTTGTCCCACCACCT	452

CD, cytosine deaminase; SDF-1, stromal cell-derived factor-1.

Sections of tumor tissues were fixed with acetone and incubated overnight with rat anti-mouse CD 31 antibody (Research Diagnostics Inc., Flanders, NJ, USA) or rabbit anti-human SDF-1 antibody (Santa Cruz Biotechnology, Inc., Santa Cruz, CA, USA) at 4°C. The sections were then incubated with FITC-conjugated anti-rabbit IgG (DAKO Japan Inc., Kyoto, Japan) or FITC-conjugated anti-rat IgG (CHEMICON INTERNATIONAL, Temecula, CA, USA) for 30 min with TO-PRO-3 iodide (Invitrogen) for nuclei labeling at room temperature. Each incubation was followed by three washes with PBS. Four color imaging was performed (Z-series, 63× oil magnification, Zeiss LSM 510-Meta Confocal Microscope; Carl Zeiss Inc., Jena, Germany). Two independent hepatologists counted the number of CD31-positive vessels of tumor tissues obtained from mice treated with PBS at day 15 ($n = 6$), only CD-TR-BME cells at day 15 ($n = 6$) and CD-TR-BME cells plus 5-FC at day 8 ($n = 6$) and day 15 ($n = 6$). In each group, 30 random fields were selected blindly.

Tissue and serum 5-FU concentrations and serum α-fetoprotein (AFP) levels. At days 8 and 15 of the experiment, tumor tissues of HuH-7 cells and sera were collected from tumor-bearing mice injected with CD-TR-BME cells and treated with 5-FC ($n = 6$). Then, 1 g of wet tumor tissue was homogenized with 1 mL of PBS. The 5-FU concentrations in the tumor tissues and sera were measured on days 8 and 15 using HPLC. In addition, to measure the serum AFP levels, tumor-bearing mice treated with CD-TR-BME cells ($n = 6$) and mice injected with CD-TR-BME cells and treated with 5-FC ($n = 6$) were killed at day 15.

Alanine aminotransferase (ALT) levels, leukocytes, hemoglobin (Hb), platelet and bodyweight. Serum ALT activity was measured using a standard UV method. Bodyweight, peripheral leukocyte count, Hb level and platelet count were also measured. The above parameters were measured at day 15.

Statistical analysis. Data were expressed as mean ± SD. Differences between groups were examined for statistical significance using the Mann–Whitney *U*-test and the Kruskal–Wallis rank test. A P-value <0.05 denoted the presence of a statistically significant difference.

Results

5-Fluorouracil inhibits cell proliferation *in vitro*. 5-Fluorouracil inhibited the proliferation of HUVEC (IC_{50}, 100.4 ng/mL) and CD-TR-BME (IC_{50}, 99.8 ng/mL) in a dose-dependent manner. However, the proliferation of HUVEC and CD-TR-BME cells was not inhibited in the presence of up to 50 ng/mL of 5-FU concentration (Fig. 1A,B). In five hepatoma cell lines, HuH-7 (IC_{50}, 10.1 ng/mL) was the most sensitive to 5-FU, followed by HAK1-B (IC_{50}, 100 ng/mL), HLF (IC_{50}, 100.4 ng/mL), KIM-1 (IC_{50}, 449.7 ng/mL) and KYN-2 (IC_{50}, 449.8 ng/mL).

CD-TR-BME cells produce 5-FU after addition of 5-FC. CD-TR-BME cells secreted 5-FU into the media and the production level was 5-FC dose dependent (Fig. 1C). After 72 h, the final

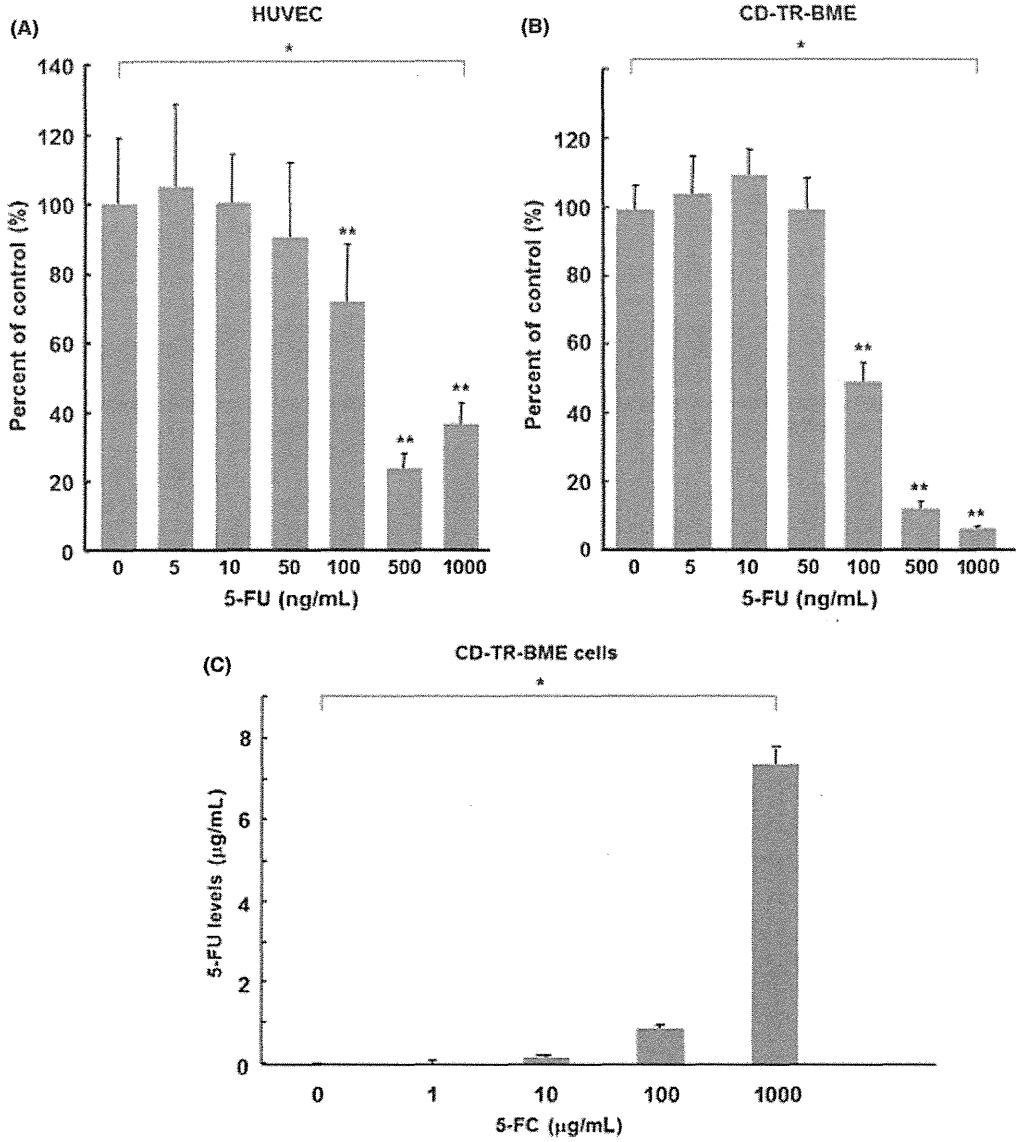

Fig. 1. Inhibition of cell proliferation by 5-fluorouracil (5-FU). (A) HUVEC, (B) CD-TR-BME. These cells were cultured with 10 mL of media containing 0–1000 ng/mL of 5-FU for 72 h. Cell proliferation was evaluated using a tetrazolium-based assay. Data are expressed relative to the control (n = 12). *P < 0.0001, using the Kruskal–Wallis test. **P < 0.0001, compared with the control group, using the Mann–Whitney U-test. (C) Secretion of 5-FU by CD-TR-BME cells with 5-fluorocytosine (5-FC). CD-TR-BME cells were cultured with 1 mL of the media containing 0–1000 mg/mL of 5-FC for 72 h. The concentration of 5-FU was measured. Data are expressed as mean ± SD of 12 samples. *P < 0.0001, using the Kruskal–Wallis test.

concentration of 5-FU secreted by the CD-TR-BME cells with 5-FC into the media was 7.4 ± 0.4 μg/mL.

"Bystander effect" of CD-TR-BME cells *in vitro*. After culture of the hepatoma cells with the chambers containing CD-TR-BME cells, the media significantly inhibited the proliferation of hepatoma cells in a 5-FC dose-dependent manner. HuH-7 was the most sensitive to 5-FC (IC_{50}, 0.89 μg/mL), followed by HAK1-B (IC_{50}, 10.3 μg/mL), KIM-1 (IC_{50}, 10.7 μg/mL), HLF (IC_{50}, 11.0 μg/mL) and KYN-2 (IC_{50}, 100.5 μg/mL) (Fig. 2). Proliferation of CD-TR-BME cells was suppressed in a 5-FC dose-dependent manner (data not shown). However, the proliferation of TR-BME cells was not suppressed with the addition of up to 1000 μg/mL 5-FC (data not shown).

Combination treatment with CD-TR-BME cells and 5-FC for a HuH-7 or KYN-2 cell xenograft model. HuH-7, the most sensitive to 5-FU, and KYN-2 cells, the most resistant, were used for *in vivo* experiments. In the HuH-7 cell xenograft model, at days 0, 3 and 6 of the initial treatment, there was no significant difference in tumor volume among the three groups. Since then, tumor volumes of the PBS-treated and CD-TR-BME groups continued to increase until day 21. From days 9 to 15, tumor growth in the CD-TR-BME + 5-FC mice was significantly suppressed compared with those of the other two groups. After completion of the 5-FC treatment, tumor volumes of CD-TR-BME + 5-FC mice started to increase rapidly and there was no significant difference in tumor volume of the three groups at day 21 (Fig. 3A,B). Serum AFP levels of the CD-TR-BME and CD-TR-BME + 5-FC mice at day 15 were 413 843 ± 203 129 and 113 436 ± 47 910 ng/mL, respectively. However, in the KYN-2 xenograft model, there was no significant difference in tumor volume among the three groups (Fig. 3C).

doi: 10.1111/j.1349-7006.2011.02182.x

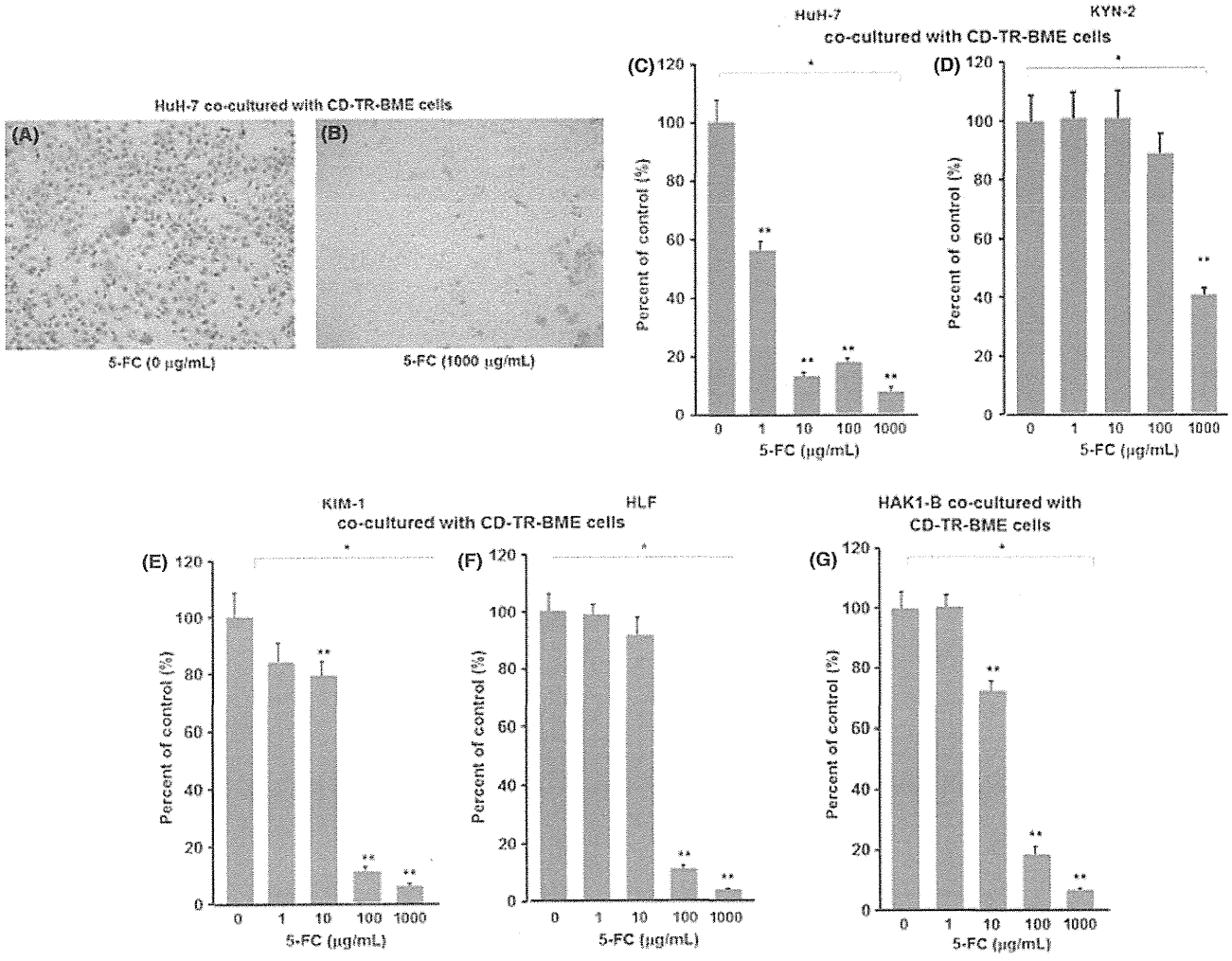

Fig. 2. Bystander effect of CD-TR-BME cells with 5-fluorocytosine (5-FC). Hepatoma cells were cultured in media containing 0–1000 mg/mL of 5-FC for 72 h with CD-TR-BME cells in chemotaxicell cell-culture chambers. (A) HuH-7 cells cultured with CD-TR-BME cells without 5-FC. (B) HuH-7 cells cultured with CD-TR-BME cells with 1000 mg/mL of 5-FC. (C–G) Cell proliferation was evaluated using a tetrazolium-based assay. Data are expressed relative to the control ($n = 12$) (C, HuH-7; D, KYN-2; E, KIM-1; F, HLF; G, HAK1-B). $*P < 0.0001$, using the Kruskal–Wallis test. $**P < 0.0001$, compared with the control group, using the Mann–Whitney *U*-test.

Migration of CD-TR-BME cells to tumor tissues and vascular density in tumor tissues. RT-PCR analysis showed SDF-1 expression in tumor tissues of HuH-7 cells and CXCR4 expression in the CD-TR-BME cells (Fig. 4A,B). Immunohistochemical analysis showed recruitment of the injected CD-TR-BME cells close to the SDF-1-expressing hepatoma cells (Fig. 4C). Examination at a higher magnification showed the incorporation of some CD-TR-BME cells into new blood vessels within the tumor tissues (Fig. 4D). However, most of these cells were localized in the interstitial tissues around the vessels in the tumor tissues (Fig. 4E). At 200-fold magnification, the numbers of CD31-positive vessels in tumor tissues of mice treated with PBS on day 15, CD-TR-BME cells on day 15 and CD-TR-BME cells plus 5-FC on days 8 and 15 were 7.2 ± 2.1, 7.2 ± 2.1, 6.9 ± 0.9 and 7.1 ± 2.1, respectively. There was no significant difference in vessel density among the groups.

5-Fluorouracil concentration in tumor tissues and sera. The 5-FU concentrations in the tumor tissues of HuH-7 cells at days 8 and 15 were 25.2 ± 14.2 and 22.4 ± 12.4 ng/mL, respectively. In all but one sample, serum 5-FU levels were not detected at days 8 and 15. Serum 5-FU concentrations of samples with detectable levels at days 8 and 15 were 8.4 and 7.3 ng/mL, respectively. These cases showed the highest tissue 5-FU concentrations at days 8 and 15, respectively.

Effect of CD-TR-BME and 5-FC treatment on leukocyte count, Hb, platelet count, serum ALT and bodyweight. Leukocyte count, Hb level and platelet count of CD-TR-BME-injected mice and CD-TR-BME + 5-FC-treated mice were 1600 ± 352/μL, 13.2 ± 1.9 g/dL, 46.3 ± 21.7 × 10^4/μL and 1800 ± 593/μL, 13.9 ± 1.2 g/dL, 48.8 ± 22.9 × 10^4/μL, respectively. Serum ALT levels of CD-TR-BME-injected mice and CD-TR-BME + 5-FC-treated mice were 38.5 ± 8.9 and 41.2 ± 7.8 U/L, respectively. The bodyweights of CD-TR-BME-injected mice and CD-TR-BME + 5-FC-treated mice were 25.2 ± 2.4 and 26.2 ± 2.9 g, respectively. There were no significant differences in leukocyte count, Hb level, platelet count, serum ALT level and bodyweight between CD-TR-BME-injected mice and CD-TR-BME + 5-FC-treated mice.

Discussion

In the *in vitro* study, HuH-7 cells were the most sensitive to 5-FU among five tested hepatoma cell lines. Furthermore, HuH-7 was more sensitive to 5-FU than CD-TR-BME cells and

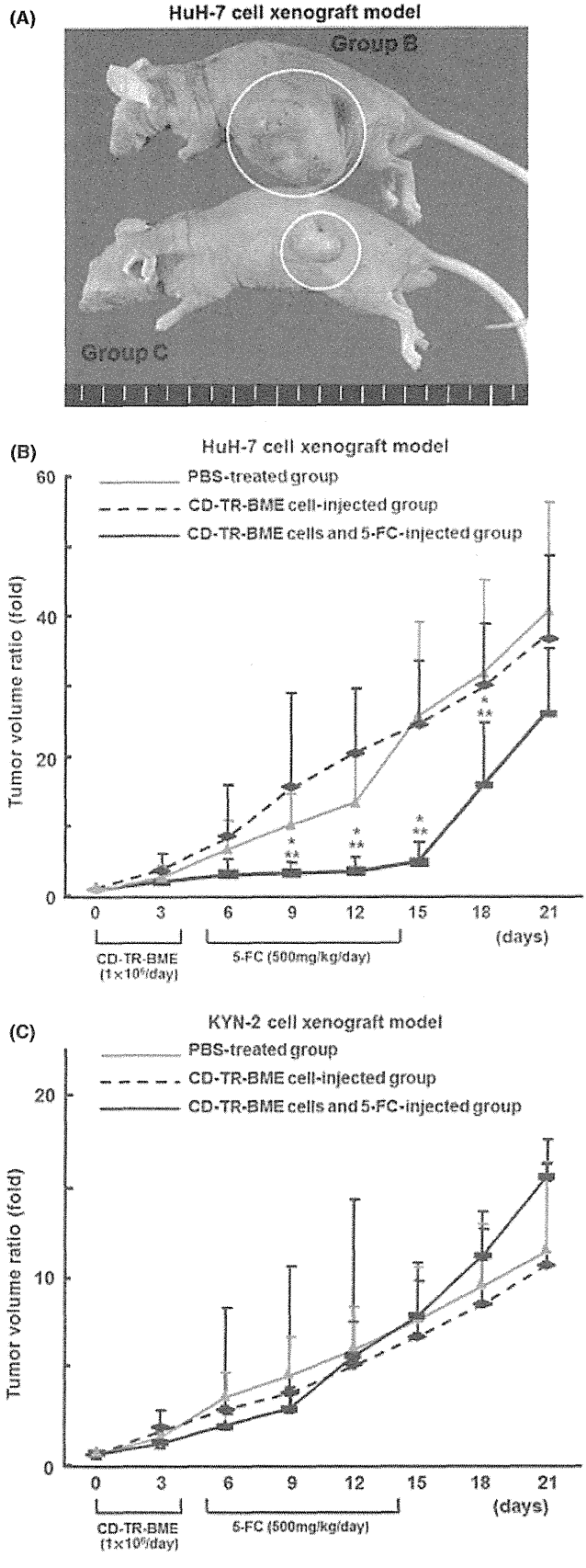

Fig. 3. Treatment of subcutaneous tumor with a combination of CD-TR-BME cells and 5-fluorocytosine (5-FC). (A) Tumors of HuH-7 cells at day 21. Group B, CD-TR-BME cells; Group C, CD-TR-BME cells + 5-FC. (B) Time-course observation of tumor volumes (HuH-7). Data are expressed relative to the control (day 0) ($n = 6$). $^*P < 0.05$, compared with the CD-TR-BME cell-injected group, using the Mann–Whitney *U*-test. $^{**}P < 0.05$, compared with PBS-treated cells, using the Mann–Whitney *U*-test. (C) Time-course observation of tumor volumes in the dorsal portion of mice (KYN-2). Data are expressed relative to the control (day 0) ($n = 6$).

HUVEC. The CD-TR-BME cells produced 5-FU into the media in a 5-FC dose-dependent manner. 5-Fluorocytosine and 5-FU are small and highly water-soluble molecules; they penetrate well into most body sites and do not require cell–cell contact for intercellular transfer.[20] CD-TR-BME cells seem to incorporate 5-FC into the cytoplasm, then produce and secrete 5-FU into the media without cell damage at relatively low concentrations of 5-FC. At higher concentrations of 5-FC, high concentrations of 5-FU in CD-TR-BME cells induce their apoptosis.

In the process of EPC homing from the bone marrow into the tumor microenvironment, vascular endothelial growth factor (VEGF) and SDF-1 undoubtedly play critical roles through specific interactions with CXCR4 and VEGFR-1 and VEGFR-2, respectively.[8,21] Recent data show that among these cytokines, VEGF mainly induces mobilization of EPC from the bone marrow into the circulation while SDF-1 recruits EPC to the tumor tissues.[22–31] In the present study, tumor tissues expressed SDF-1 and CD-TR-BME cells expressed CXCR4. Injected CD-TR-BME cells migrated to tumor tissues. Of course, there seems to be a possibility that some of the injected CD-TR-BME cells have migrated to other tissues such as non-cancerous liver tissue and bone marrow. Tamura *et al.*[23] reported that intravenously injected TR-BME cells were homed to tumor tissue with significantly higher specificity. Injected CD-TR-BME cells seemed to migrate mainly to tumor tissues through SDF-1 and CXCR4 interaction.

Interestingly, some of the injected CD-TR-BME cells were incorporated into vascular formation and others were distributed in the interstitial space of tumor tissue. Furthermore, intravenous injection of CD-TR-BME cells did not increase the vascular density in tumor tissues. These distribution patterns were also observed in tumor tissues with the injection of wild type EPC in our preliminary study. Another group reported that only some of the systemically injected EPC were incorporated into tumor vessels.[8] A wide range of cell types including endothelial cells were shown to transdifferentiate into tumor-associated-fibroblasts (TAF).[24] Residual CD-TR-BME cells might migrate to the interstitial space due to the enhanced permeability of tumor vessels and transdifferentiate into TAF.[25] In general, tumor tissues produce VEGF and SDF-1 to recruit an appropriate number of bone marrow-derived EPC for vasculogenesis.[2,4] We might have injected too many CD-TR-BME cells than what was required for vasculogenesis.

The concentrations of 5-FU in tumor tissues on days 8 and 15 of the treatment were 25.4 ± 13.0 and 22.4 ± 12.4 ng/g wet tissue, respectively. Serum 5-FU was not detected in any of the samples except for one on days 8 and 15, respectively. As the CD-TR-BME cells and EPC selectively migrate to tumor tissues, we assume that 5-FU was selectively produced by the CD-TR-BME cells in tumor tissues. Therefore, no adverse effects were observed. Treatment with 5-FC after CD-TR-BME cell injection did not reduce the vascular density in tumor tissues. In the *in vitro* study, proliferation of HUVEC and CD-TR-BME cells was not suppressed in the presence of up to 50 ng/mL of 5-FU, while proliferation of HuH-7 cells was suppressed by 36 and 52% at 10 and 50 ng/mL of 5-FU, respectively. The CD/5-FC system mainly suppressed tumor growth of HuH-7 cells in

doi: 10.1111/j.1349-7006.2011.02182.x

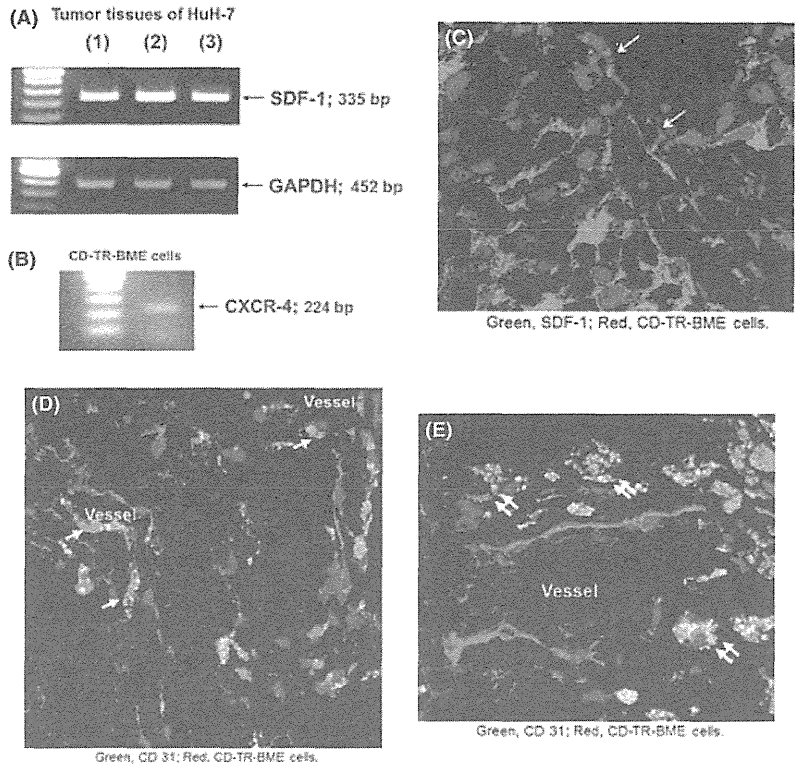

Fig. 4. Migration of CD-TR-BME cells to tumor tissues. (A) Expression of stromal-derived factor-1 (SDF-1) transcripts in tumor tissues (RT-PCR). Lanes 1–3, representative tumor tissues of HuH-7 cells. (B) Expression of CXCR4 transcripts in CD-TR-BME cells (RT-PCR). (C–E) Immunostaining of SDF-1 (green) and CD31 (green) with nuclear staining (blue) in tumor tissues of mice injected with CD-TR-BME cells labeled with red fluorescent marker PKH26-red. CD-TR-BME cells (red) (arrows) were recruited to tumor tissue close to SDF-1-expressing hepatoma cells (green) (C). CD-TR-BME cells (red) were incorporated into vessel walls (arrows) (D) or distributed within stromal tissue near a blood vessel (double arrows) (E).

the xenograft model by inhibiting tumor cell proliferation rather than an anti-angiogenic effect. However, The CD/5-FC system seems to be unable to maintain enough concentration of 5-FU to suppress the tumor growth of KYN-2 cells, which are 5-FU resistant. In the *in vitro* study, HuH-7 cells were more sensitive to 5-FU than KYN-2 cells. Since cell proliferation of KYN-2 cells was not suppressed in the presence of up to 100 ng/mL of 5-FU, the 5-FU concentration in tumor tissues seemed too low to suppress the tumor growth of KYN-2 cells *in vivo*. Miller *et al.*[26] reported that inherent 5-FU sensitivity is an important factor in determining efficacy of the CD/5-FC system. These findings indicate that diffusible 5-FU from CD-TR-BME cells in tumor tissues is at an optimal concentration to suppress the proliferation of HuH-7 cells. Furthermore, as the concentration of 5-FU in tumor tissues on day 15 of the treatment was maintained similar to that on day 8, the number of injected CD-TR-BME cells in tumor tissues did not seem to be decreased by the 5-FU produced by these cells.

Our CD/5-FC system with carrier cells enabled gene delivery to tumor tissues and repeated treatment by the escape from anti-vector immunity. However, for clinical application, the following issues must be resolved. First, the injected cells must be improved for more selective migration to tumor tissues. To improve selective migration to tumor tissues, gene transfection of CXCR4 or VEGF receptor (VEGFR) to CD-TR-BME cells might be necessary. Second, production of 5-FU in tumor tissues must be upregulated. To upregulate 5-FU production in tumor tissues, it might be necessary to increase the number of injected CD-TR-BME cells or to transfect more CD cDNA to TR-BME cells. However, high concentrations of 5-FU in tumor tissues induced apoptosis of CD-TR-BME cells as well as tumor cells. Repeated injections of CD-TR-BME cells will be required. The other possible way is to use a replication-competent oncolytic virus as the vector.[27,28] The replication-competent virus vector will be able to transfect CD cDNA to tumor cells and other kinds of cells in tumor tissues and upregulate 5-FU production. Third, tumor cell proliferation by injected CD-TR-BME cells must be inhibited. There were no significant differences in tumor volume and vascular density between the non-treated tumor group and the CD-TR-BME cell-injected tumor group. Furthermore, Sasajima *et al.*[29] reported that injection of vascular proangiogenic cells caused vascular remodeling and delay of tumor growth as well as a reduction of factors involved in drug resistance. As EPC produce VEGF, EGF, TGF-α and HGF,[30,31] these growth factors might stimulate tumor cell proliferation and angiogenesis.

In conclusion, we have demonstrated that injected CD cDNA-transfected endothelial progenitor cell lineage migrated to the tumor tissues of hepatoma cells and suppressed tumor growth by producing 5-FU in tumor tissues with intraperitoneal 5-FC injection. Our CD/5-FC system did not cause any severe adverse effects, suggesting that selective 5-FU production in tumor tissues with the character of EPC to home to tumor tissues might be a suitable strategy in the treatment of human HCC.

Acknowledgment

The authors thank Professor D. F. Condorelli for his kind supply of the *E. coli* CD gene (pLXSP-CD).

Disclosure Statement

The authors have no commercial affiliations and no financial relationships to disclose.

References

1 Asahara T, Murohara T, Isner JM *et al.* Isolation of putative progenitor endothelial cells for angiogenesis. *Science* 1997; **275**: 964–7.
2 Isner JM, Kalka C, Kawamoto A, Asahara T. Bone marrow as a source of endothelial cells for natural and iatrogenic vascular repair. *Ann NY Acad Sci* 2001; **953**: 75–84.
3 Vajkoczy P, Blum S, Hatzopoulos AK *et al.* Multistep nature of microvascular recruitment of *ex vivo*-expanded embryonic endothelial progenitor cells during tumor angiogenesis. *J Exp Med* 2003; **197**: 755–65.
4 Dome B, Hendrix MJ, Paku S, Tovari J, Timar J. Alternative vascularization mechanisms in cancer: pathology and therapeutic implications. *Am J Pathol* 2007; **170**: 1–15.
5 Folkman J. Tumor angiogenesis in women with node-positive breast cancer. *Cancer J Sci Am* 1995; **1**: 106–8.
6 Jin H, Aiyer A, Varner J *et al.* A homing mechanism for bone marrow-derived progenitor cell recruitment to the neovasculature. *J Clin Invest* 2006; **116**: 652–62.
7 Bagley RG, Weber W, Rouleau C, Teicher BA. Pericytes and endothelial precursor cells: cellular interactions and contributions to malignancy. *Cancer Res* 2005; **65**: 9741–50.
8 Orimo A, Gupta PB, Weinberg RA *et al.* Stromal fibroblasts present in invasive human breast carcinomas promote tumor growth and angiogenesis through elevated SDF-1/CXCL12 secretion. *Cell* 2005; **121**: 335–48.
9 Polak A, Scholer HJ. Mode of action of 5-fluorocytosine and mechanisms of resistance. *Chemotherapy* 1975; **21**: 113–30.
10 Dong Y, Wen P, Fine HA *et al.* *In vivo* replication-deficient adenovirus vector-mediated transduction of the cytosine deaminase gene sensitizes glioma cells to 5-fluorocytosine. *Hum Gene Ther* 1996; **7**: 713–20.
11 Kuriyama S, Kikukawa M, Tsujii T *et al.* Cytosine deaminase/5-fluorocytosine gene therapy can induce efficient anti-tumor effects and protective immunity in immunocompetent mice but not in athymic nude mice. *Int J Cancer* 1999; **81**: 592–7.
12 Di Bisceglie AM, Rustgi VK, Hoofnagle JH, Dusheiko GM, Lotze MT. NIH conference. Hepatocellular carcinoma. *Ann Intern Med* 1988; **108**: 390–401.
13 Matsui O, Kadoya M, Ida M *et al.* Benign and malignant nodules in cirrhotic livers: distinction based on blood supply. *Radiology* 1991; **178**: 493–7.
14 Honda H, Tajima T, Masuda K *et al.* Vascular changes in hepatocellular carcinoma: correlation of radiologic and pathologic findings. *AJR* 1999; **173**: 1213–7.
15 Ando E, Tanaka M, Sata M *et al.* Hepatic arterial infusion chemotherapy for advanced hepatocellular carcinoma with portal vein tumor thrombosis: analysis of 48 cases. *Cancer* 2002; **95**: 588–95.
16 Han KH, Seong J, Kim JK, Ahn SH, Lee DY, Chon CY. Pilot clinical trial of localized concurrent chemoradiation therapy for locally advanced hepatocellular carcinoma with portal vein thrombosis. *Cancer* 2008; **113**: 995–1003.
17 Hattori K, Muta M, Nakashima E *et al.* Establishment of bone marrow-derived endothelial cell lines from ts-SV40 T-antigen gene transgenic rats. *Pharm Res* 2001; **18**: 9–15.
18 Garber JC, Barbee RW. *Guide for the care and use of laboratory animals.* 1996 edn. Washington DC: The National Academies Press, 2000, 1–220.
19 Barresi V, Belluardo N, Sipione S, Mudo G, Cattanes E, Condorelli DF. Transplantation of prodrug-converting neural progenitor cells for brain tumor therapy. *Cancer Gene Ther* 2003; **10**: 396–402.
20 Haberkorn U, Oberdorfer F, Schackert HK *et al.* Monitoring gene therapy with cytosine deaminase: *in vitro* studies using tritiated-5-fluorocytosine. *J Nucl Med* 1996; **37**: 87–94.
21 Li B, Sharpe EE, Young PP *et al.* VEGF and PlGF promote adult vasculogenesis by enhancing EPC recruitment and vessel formation at the site of tumor neovascularization. *FASEB J* 2006; **20**: 1495–7.
22 Aghi M, Cohen KS, Klein RJ, Scadden DT, Chiocca EA. Tumor stromal-derived factor-1 recruits vascular progenitors to mitotic neovasculature, where microenvironment influences their differentiated phenotypes. *Cancer Res* 2006; **66**: 9054–64.
23 Tamura M, Unno K, Oku N *et al.* *In vivo* trafficking of endothelial progenitor cells their possible involvement in the tumor neovascularization. *Life Sci* 2004; **75**: 575–84.
24 Xouri G, Christian S. Origin and function of tumor stroma fibroblasts. *Semin Cell Dev Biol* 2010; **21**: 40–6.
25 Matsumura Y, Kataoka K. Preclinical and clinical studies of anticancer agent-incorporating polymer micelles. *Cancer Sci* 2009; **100**: 572–9.
26 Miller CR, Williams CR, Buchsbaum DJ, Gillespie GY. Intratumoral 5-fluorouracil produced by cytosine deaminase/5-fluorocytosine gene therapy is effective for experimental human glioblastomas. *Cancer Res* 2002; **62**: 773–80.
27 Power AT, Bell JC. Cell-based delivery of oncolytic viruses: a new strategic alliance for a biological strike against cancer. *Mol Ther* 2007; **15**: 660–5.
28 Willmon C, Harrington K, Kottke T, Prestwich R, Melcher A, Vile R. Cell carriers for oncolytic viruses: Fed Ex for cancer therapy. *Mol Ther* 2009; **17**: 1667–76.
29 Sasajima J, Mizukami Y, Kohgo Y *et al.* Transplanting normal vascular proangiogenic cells to tumor-bearing mice triggers vascular remodeling and reduces hypoxia in tumors. *Cancer Res* 2010; **70**: 6283–92.
30 Taniguchi E, Kin M, Torimura T *et al.* Endothelial progenitor cell transplantation improves the survival following liver injury in mice. *Gastroenterology* 2006; **130**: 521–31.
31 Nakamura T, Torimura T, Sata M *et al.* Significance and therapeutic potential of endothelial progenitor cell transplantation in a cirrhotic liver rat model. *Gastroenterology* 2007; **133**: 91–107.

doi: 10.1111/j.1349-7006.2011.02182.x

World Journal of Gastroenterology

Online Submissions: http://www.wjgnet.com/1007-9327office
wjg@wjgnet.com
doi:10.3748/wjg.v18.i28.3673

World J Gastroenterol 2012 July 28; 18(28): 3673-3680
ISSN 1007-9327 (print) ISSN 2219-2840 (online)

ORIGINAL ARTICLE

Intraductal neoplasm of the intrahepatic bile duct: Clinicopathological study of 24 cases

Yoshiki Naito, Hironori Kusano, Osamu Nakashima, Eiji Sadashima, Satoshi Hattori, Tomoki Taira, Akihiko Kawahara, Yoshinobu Okabe, Kazuhide Shimamatsu, Jun Taguchi, Seiya Momosaki, Koji Irie, Rin Yamaguchi, Hiroshi Yokomizo, Michiko Nagamine, Seiji Fukuda, Shinichi Sugiyama, Naoyo Nishida, Koichi Higaki, Munehiro Yoshitomi, Masafumi Yasunaga, Koji Okuda, Hisafumi Kinoshita, Masamichi Nakayama, Makiko Yasumoto, Jun Akiba, Masayoshi Kage, Hirohisa Yano

Yoshiki Naito, Hironori Kusano, Osamu Nakashima, Masamichi Nakayama, Makiko Yasumoto, Jun Akiba, Hirohisa Yano, Departments of Pathology, Kurume University School of Medicine, Kurume 830-0011, Japan
Eiji Sadashima, Satoshi Hattori, Biostatistics Center, Kurume University, Kurume 830-0011, Japan
Tomoki Taira, Akihiko Kawahara, Masayoshi Kage, Department of Diagnostic Pathology, Kurume University Hospital, Kurume 830-0011, Japan
Yoshinobu Okabe, Division of Gastroenterology, Department of Medicine, Kurume University School of Medicine, Kurume 830-0011, Japan
Kazuhide Shimamatsu, Department of Pathology, Omuta City General Hospital, Omuta 836-8567, Japan
Jun Taguchi, Department of Pathology, Asakura Medical Association Hospital, Fukuoka 838-0069, Japan
Seiya Momosaki, Department of Pathology, National Hospital Organization Kyushu Medical Center, Fukuoka 810-8563, Japan
Koji Irie, Department of Pathology, Shin-Koga Hospital, Tenjinkai, 120 Tenjincho, Kurume 830-0033, Japan
Rin Yamaguchi, Department of Pathology, Kurume University Medical Center, 155-1 Kokubumachi, Kurume 839-0863, Japan
Hiroshi Yokomizo, Department of Surgery, Japanese Red Cross Kumamoto Hospital, Kumamoto 861-8520, Japan
Michiko Nagamine, Seiji Fukuda, Department of Pathology, Japanese Red Cross Kumamoto Hospital, Kumamoto 861-8520, Japan
Shinichi Sugiyama, Division of Surgery, Saiseikai Kumamoto Hospital, Kumamoto 861-4193, Japan
Naoyo Nishida, Koichi Higaki, Department of Pathology, St Mary's Hospital, Kurume 830-8543, Japan
Munehiro Yoshitomi, Masafumi Yasunaga, Koji Okuda, Hisafumi Kinoshita, Department of Surgery, Kurume University School of Medicine, Kurume 830-0011, Japan
Author contributions: Naito Y, Nakashima O and Kusano H performed the majority of the experiments; Yano H was involved in editing the manuscript; all authors provided the collection of all the human material and advised for the manuscript.
Correspondence to: Yoshiki Naito, MD, PhD, Department of Pathology, Kurume University School of Medicine, 67 Asahimachi, Kurume 830-0011, Japan. nyoshiki@med.kurume-u.ac.jp
Telephone: +81-942-317546 Fax: +81-942-320905
Received: November 14, 2011 Revised: March 27, 2012
Accepted: March 29, 2012
Published online: July 28, 2012

Abstract

AIM: To investigate the clinicopathological features of intraductal neoplasm of the intrahepatic bile duct (INihB).

METHODS: Clinicopathological features of 24 cases of INihB, which were previously diagnosed as biliary papillomatosis or intraductal growth of intrahepatic biliary neoplasm, were reviewed. Mucin immunohistochemistry was performed for mucin (MUC)1, MUC2, MUC5AC and MUC6. Ki-67, P53 and β-catenin immunoreactivity were also examined. We categorized each tumor as adenoma (low grade), borderline (intermediate grade), and malignant (carcinoma *in situ*, high grade including tumors with microinvasion).

RESULTS: Among 24 cases of INihB, we identified 24 tumors. Twenty of 24 tumors (83%) were composed of a papillary structure; the same feature observed in intraductal papillary neoplasm of the bile duct (IPNB). In contrast, the remaining four tumors (17%) showed both tubular and papillary structures. In three of the four tumors (75%), macroscopic mucin secretion was limited but microscopic intracellular mucin was evident. Histologically, 16 tumors (67%) were malignant, three (12%) were borderline, and five (21%) were adenoma. Microinvasion was found in four cases (17%). Immunohistochemical analysis revealed that MUC1 was not expressed in the borderline/adenoma group but was

expressed only in malignant lesions (P = 0.0095). Ki-67 labeling index (LI) was significantly higher in the malignant group than in the borderline/adenoma group (22.2 ± 15.5 *vs* 7.5 ± 6.3, P < 0.01). In the 16 malignant cases, expression of MUC5AC showed borderline significant association with high Ki-67 LI (P = 0.0622). Nuclear expression of β-catenin was observed in two (8%) of the 24 tumors, and these two tumors also showed MUC1 expression. P53 was negative in all tumors.

CONCLUSION: Some cases of INihB have a tubular structure, and are subcategorized as IPNB with tubular structure. MUC1 expression in INihB correlates positively with degree of malignancy.

Key words: Intraductal biliary neoplasm; Intraductal papillary neoplasm of the bile duct; Intraductal tubular neoplasm of the bile duct; Intraductal tubulopapillary neoplasm of the bile duct; Mucin expression

Peer reviewer: Dr. George Sgourakis, 2nd Surgical Department, Surgical Oncology Unit, Red Cross Hospital, 11 Mantzarou Str, 15451 Athens, Greece

Naito Y, Kusano H, Nakashima O, Sadashima E, Hattori S, Taira T, Kawahara A, Okabe Y, Shimamatsu K, Taguchi J, Momosaki S, Irie K, Yamaguchi R, Yokomizo H, Nagamine M, Fukuda S, Sugiyama S, Nishida N, Higaki K, Yoshitomi M, Yasunaga M, Okuda K, Kinoshita H, Nakayama M, Yasumoto M, Akiba J, Kage M, Yano H. Intraductal neoplasm of the intrahepatic bile duct: Clinicopathological study of 24 cases. *World J Gastroenterol* 2012; 18(28): 3673-3680 Available from: URL: http://www.wjgnet.com/1007-9327/full/v18/i28/3673.htm DOI: http://dx.doi.org/10.3748/wjg.v18.i28.3673

INTRODUCTION

Mucin-producing tumors arising from the bile duct have been reported previously[1-5], but as a disease category, consensus has not yet been reached. Recently, Shibahara *et al*[6] and Zen *et al*[7] have contributed to the development of the concept of papillary tumors in the bile duct that resemble intraductal papillary mucinous neoplasm of the pancreas (IPMN-P) and pancreatic intraepithelial neoplasia. These bile duct tumors show papillary proliferation in the bile duct with mucin secretion, and are considered as intraductal papillary neoplasm of the bile duct (IPN-B), that is, the biliary counterpart of IPMN-P[8,9]. Recent studies have indicated that IPN-B could be subcategorized according to the results of mucin immunohistochemistry[6,7], and the similarity of IPNB and IPMN-P has also been described.

In our current study, we conducted histological and immunohistochemical re-examination of 24 cases of intraductal neoplasm of the intrahepatic bile duct (INihB), which were previously reported as biliary papillomatosis or intraductal growth type of intrahepatic biliary neoplasm[10-13].

MATERIALS AND METHODS

Definition of INihB

We defined INihB as a tumor that (1) was localized in the liver; (2) arose within the intrahepatic bile duct; (3) had a major lesion that was noninfiltrative and showed an intraductal proliferation pattern; and (4) clinicopathologically communicated with the surrounding bile duct.

Tissue samples

We identified 24 cases of INihB from the medical record at Kurume University Hospital and affiliated institutions. These cases were previously diagnosed as intraductal intrahepatic biliary neoplasm or biliary papillomatosis[13]. Tissue sections of 4 μm thickness were prepared from paraffin-embedded tissue samples, and stained with hematoxylin and eosin (HE) in the usual manner. The slides were reviewed by the three pathologists (YN, HK and ON).

Degree of malignancy of intrahepatic bile duct

HE-stained sections were reviewed and each tumor was categorized into three groups according to the degree of malignancy by using the criteria in IPMN-P[8]: adenoma (low grade), borderline (intermediate grade), and malignant (carcinoma *in situ* and high grade). Tumors with microinvasion were categorized as malignant.

Immunohistochemistry

Paraffin-embedded, 4-μm-thick sections on a coated glass slides were stained by using the BenchMark XT (Ventata Automated Systems, Inc., Tucson, AZ, United States) with the following antibodies: mucin (MUC)1 (mouse monoclonal, Ma695, dilution 1:100; Novocastra, Newcastle, United Kingdom); MUC2 (mouse monoclonal, Ccp58, dilution 1:100; Novocastra); MUC5AC (mouse monoclonal, CLH2, dilution 1:100; Novocastra); MUC6 (mouse monoclonal, CLH5, dilution 1:50; Novocastra); p53 (mouse monoclonal, DO-7, dilution 1:200; Novocastra); β-catenin (mouse monoclonal, β-catenin-1, dilution 1:200; Dako, Glostrup, Denmark); and Ki-67 (mouse monoclonal, MIB-1, dilution 1:100; Dako). This automated system uses the streptavidin-biotin complex method with DAB as a chromogen (Ventana iVIEW DAB Detection Kit).

Regarding the MUC profile, we evaluated cytoplasmic and luminal surface staining by referring to the method of Shibahara *et al*[6], and the cells were considered positive when either one or both of the two components were stained. The percentage of positively stained neoplastic cells was also calculated and graded as follows: -, < 5% of the neoplastic cells were stained; +, ≥ 5% and < 20% were stained; 2+, ≥ 20% and < 50% were stained, and 3+, ≥ 50% were stained. These evaluations were conducted by three pathologists (YN, HK and ON). Positivity of p53 and β-catenin were defined by distinct and diffuse nuclear staining among the neoplastic cells. Ki-67 staining was counted on a minimum of 1000 tumor cells and Ki-67 labeling index (LI) was calculated as the per-

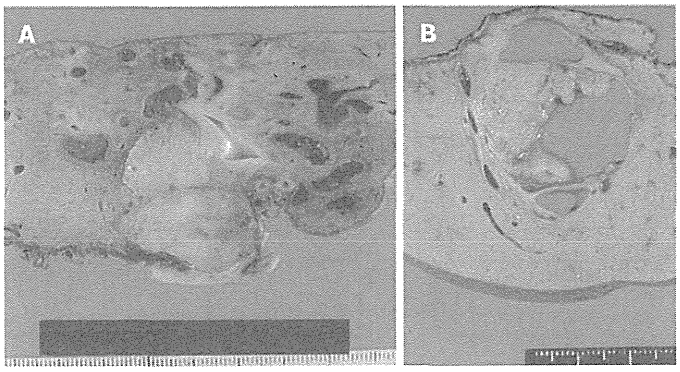

Figure 1 Gross findings. A: Duct-ectatic type. Tumor filled the dilated intrahepatic bile duct. Surrounding bile duct was also dilated; B: Cystic type. Cystic dilatation of intrahepatic bile duct. Papillary tumor was found in the dilated intrahepatic bile duct. Significant retention of mucin was observed.

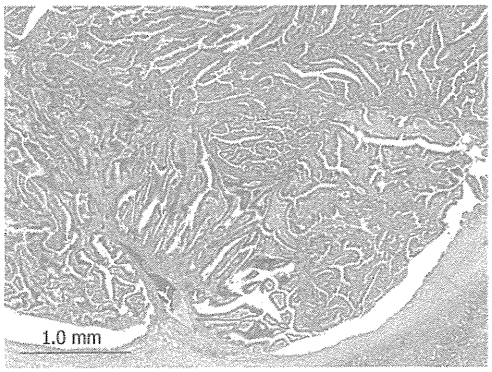

Figure 2 Histopathology of intraductal neoplasm of the intrahepatic bile duct. Tumor shows papillary proliferation within the dilated bile duct (hematoxylin and eosin stain, × 20).

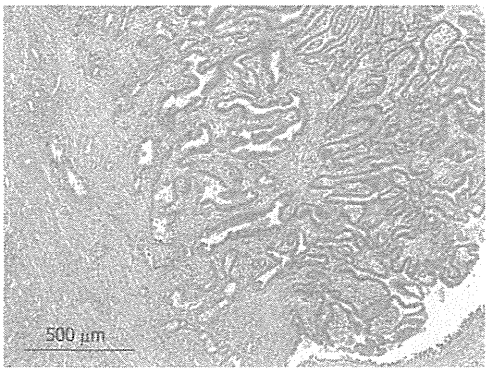

Figure 3 Microinvasion of tumor. Tumor cells infiltrating into the bile duct wall (hematoxylin and eosin stain, × 40).

centage of positively stained cells to total cells.

Statistical analysis

Associations of Ki-67 LI and expression of MUC family (0, 1+ or 2+, 3+) with the degree of malignancy (adenoma, borderline or malignant), and association between Ki-67 LI and MUC profile were examined using the Kruskal-Wallis test and Fisher's exact test. To apply Fisher's exact test, we classified MUC profile into two categories of 0 or 1+ and 2+ or 3+. Association was considered significant when $P < 0.05$. All the statistical analyses were conducted by SAS version 9.12 (SAS Institute Inc., Cary, NC, United States) and R version 2.9.0.

RESULTS

Patients with INihB

We identified 24 tumors in 24 patients. Clinical findings are summarized in Table 1. Median age at the initial diagnosis was 64 years (mean: 63.0 ± 8.1), and the male: female ratio was 1:1. Sixteen tumors (67%) were located in the left lobe. Nineteen tumors (79%) were cystic type associated with mucin hypersecretion, and five tumors (21%) were duct-ectatic type without mucin hypersecretion (Figure 1). Twenty tumors (83%) had papillary structures in the bile duct as IPNB (Figure 2). The remaining four tumors (17%) presented the following features: the tumor was localized and proliferated in the bile duct, and the tumor showed both tubular and papillary structures. In three of the four tumors (75%), macroscopic mucin secretion was limited but microscopic intracellular mucin was evident. Histologically, 16 tumors (67%) were malignant, three (12%) were borderline, and five (21%) were adenoma. Microinvasion was found in four tumors (21%) (Figure 3), and these were categorized as malignant. There was no ovarian-like stroma in any cases.

Four tumors (17%) were composed of both papillary and tubular structures (Table 2). Histological findings of four patients were similar to those of intraductal tubulopapillary neoplasm (ITPN-P)[14] or intraductal tubular neoplasm of the pancreas (ITN-P)[15]. One of these four cases was previously reported as a biliary papillomatosis by Taguchi *et al*[13], and the tumor spread from the intrahepatic to extrahepatic bile duct. Another two cases also showed extension of tumor with bile duct dilation. However, the remaining tumor was cystic type and macroscopic mucin hypersecretion was evident. Among tubular structures, a pyloric gland-like structure (Figure 4) was prominent. Three cases were not malignant, but one tumor showed cytological atypia, such as enlarged nuclei with pleomorphism, and was considered as malignant (Figure 5). Atypi-

Table 1 Clinicopathological features of 24 patients with intraductal neoplasm of the intrahepatic bile duct

Age (yr), median (mean ± SD)	64.0 (63.0 ± 8.1)
Gender, *n* (%)	
Male	12 (50)
Female	12 (50)
Location, *n* (%)	
Left lobe	16 (67)
Right lobe	8 (33)
Tumor size (cm), median (mean ± SD)	30 (42.2 ± 26.6)
Macroscopic findings of bile duct, *n* (%)	
Duct-ectatic	5 (21)
Cystic	19 (79)
Macroscopic mucin hypersecretion, *n* (%)	
Present	19 (79)
Absent	5 (21)
Histological structure pattern, *n* (%)	
Papillary	20 (83)
Tubular and papillary	4 (17)
Histological grade, *n* (%)	
Malignant	16 (67)
Borderline	3 (12)
Adenoma	5 (21)
Microinvasion, *n* (%)	
Present	4 (17)
Absent	20 (83)

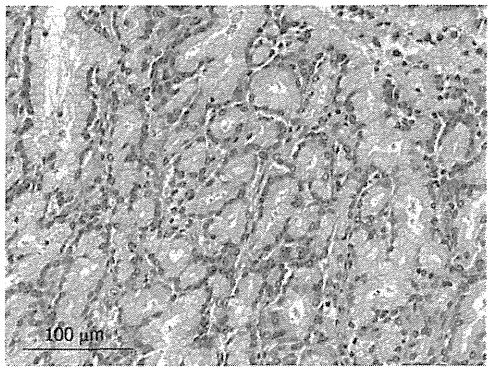

Figure 4 Tubular structure within intraductal neoplasm of the intrahepatic bile duct. Cells with intracellular mucin and mild atypia forming a pyloric gland-like structure (hematoxylin and eosin stain, × 200).

cal cells lining the tubular structure were cuboidal or columnar with little or no cytoplasmic mucin. None of these four cases were associated with tumor invasion.

Immunohistochemical analysis of INihB

Immunohistochemical findings are shown in Table 3. MUC1 was not expressed in the borderline/adenoma group but was expressed in malignant lesions ($P = 0.0095$). No specific pattern of expression was observed for other MUC family members. The Ki-67 LI was significantly higher in the malignant group than in the borderline/adenoma group (22.2 ± 15.5 *vs* 7.5 ± 6.3, $P < 0.01$, Figure 6A). In the 16 malignant tumors, there was an association of borderline significance between expression of MUC5AC and higher Ki-67 LI ($P = 0.0622$, Figure 6B). Expression of β-catenin was found in two of the 24 tumors (8%, Figure 7), and these two tumors were also positive for MUC1. P53 was negative in all 24 tumors.

Table 2 Clinicopathological findings of intraductal neoplasm of the intrahepatic bile duct with papillary and tubular structure in four patients

	Case 1	Case 2	Case 3[1]	Case 4
Age (yr)	77	49	63	52
Gender	Male	Female	Male	Male
Location	Left lobe			
Tumor size (cm)	10	2	6	2.6
Mucin produced macroscopically	Absent			Present
Macroscopic findings	Duct-ectatic type			Cystic
Histopathological grade	Malignant	Borderline	Adenoma	Adenoma
Microinvasion	Absent			
Mucin immunohistochemistry				
MUC1	3+	-	-	1+
MUC2	-	-	-	-
MUC5AC	-	1+	-	-
MUC6	3+	3+	+	3+

[1]Has been reported as biliary papillomatosis.

Table 3 Immunohistochemical features of 24 cases of intraductal neoplasm of the intrahepatic bile duct

	Malignant *n* (16.67%)	Borderline *n* (3.12%)/ adenoma *n* (5.21%)
MUC1[1]		
3+ (38%)	9 (56)	0
2+ (0%)	0	0
1+/- (62%)	7 (44)	8 (100)
MUC2		
3+ (13%)	1 (6)	2 (25)
2+ (4%)	1 (6)	0
1+/- (83%)	14 (88)	6 (75)
MUC5AC		
3+ (46%)	7 (44)	4 (50)
2+ (12%)	2 (12)	1 (13)
1+/- (42%)	7 (44)	3 (37)
MUC6		
3+ (46%)	4 (25)	5 (63)
2+ (12%)	4 (25)	1 (22)
1+/- (44%)	8 (50)	2 (25)
Proliferation		
Ki-67 (LI, %, mean ± SD)[2]	22.2 ± 15.5	7.5 ± 6.3
Genetic status		
TP53 overexpression	0	0
β-catenin nuclear expression (17%)[3]	2 (13)	0

[1]MUC1 expression was exhibited only in the malignant group ($P = 0.0095$); [2]Ki-67 was significantly higher in malignant cases than in borderline/adenoma patients ($P < 0.01$); [3]β-catenin expression was observed only in the cases with MUC1 expression. LI: Labeling index.

DISCUSSION

Many studies have been conducted on IPMN-P, and histomorphological criteria for diagnosis have been determined[8]. Regarding similar lesions in the bile duct, the definition of IPNB[7] and mucin-producing bile duct tumors[6] is proposed as a new conceptual framework

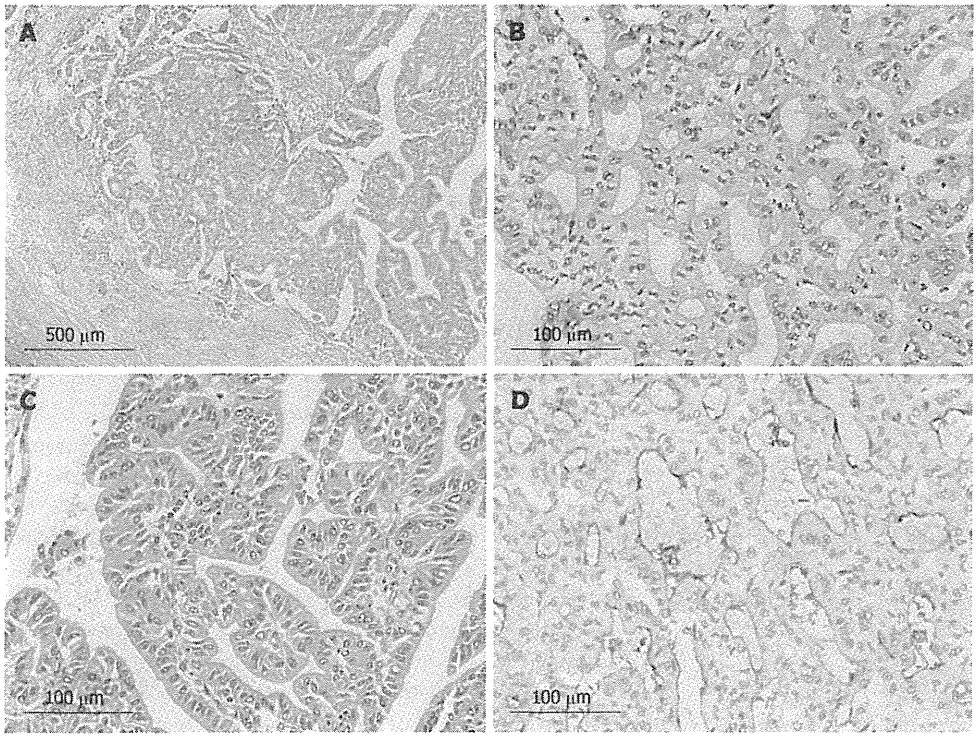

Figure 5 Histology of intraductal neoplasm of the intrahepatic bile duct with papillary and tubular structure (case 1). A: Histological structure was mainly tubular, but papillary structure was also present [hematoxylin and eosin (HE) stain, × 40]; B: Tubular structure (HE stain, × 200); C: Papillary structure (HE stain, × 200); D: Tumor cells were positive for mucin (MUC)1 immunohistochemistry (MUC1 stain, × 200).

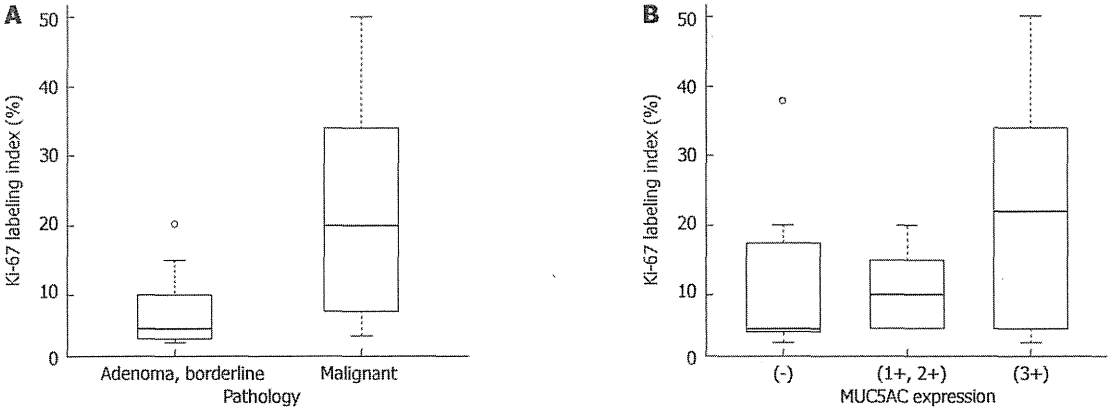

Figure 6 Box plot for Ki-67 labeling index by histological degree of malignancy and MUC5AC expression. A: The Ki-67 labeling index (LI) was significantly higher in the malignant group than in the benign/borderline group; B: There was an association with borderline significance between MUC5AC expression and Ki-67 LI (P = 0.0622). MUC: Mucin.

of biliary intraductal neoplasms. These biliary lesions present the same histological features of IPMN-P, and Zen *et al*[16,17] divided them into four categories, namely, pancreaticobiliary type, intestinal type, gastric type, and oncocytic type. In contrast, Shibahara *et al*[6] subclassified the lesions into two distinct categories, namely, columnar type and cuboidal type. Columnar type resembles intestinal type, and cuboidal type resembles pancreaticobiliary type or intraductal oncocytic papillary neoplasm, and they hypothesized that these two categories could be the biliary counterparts of IPMN-P.

Among our 24 cases of INihB, 19 cases (79%) were the cystic type that was proposed by Shibahara *et al*[6], and this type is known as a biliary cystic tumor. Devaney *et al*[18] reported that ovarian-like stroma was observed in 85% of the adenoma and 28% of the adenocarcinoma tumors. However, none of our cases had ovarian-like stroma. The presence or absence of ovarian-like stroma is an important factor for the classification of IPNB. Recently, Zen *et al*[17] proposed that biliary cystic tumor could be a cystic variant of IPNB, having bile duct communication and absence of ovarian-like stroma. Based on our

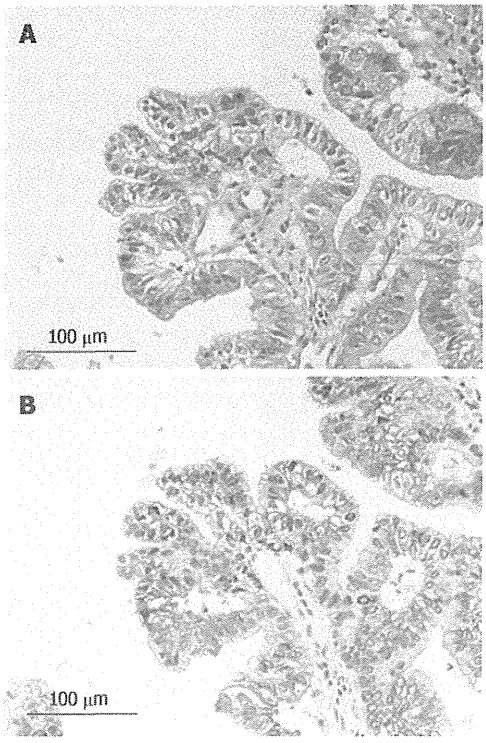

Figure 7 Nuclear expression of β-catenin in pancreaticobiliary type. A: Hematoxylin and eosin stain, × 200; B: β-catenin stain, × 200.

findings, the cystic type reported by Shibahara *et al*[6] and biliary cystic variant of IPNB reported by Zen *et al*[16] are the most common type among INihB, and they can be recognized by their characteristic macroscopic findings, that is, a cystic change with mucin hypersecretion, even though the tumors have ovarian-like stroma.

In our current study, 20 of 24 INihB tumors (83%) showed purely papillary proliferation that is a morphological feature of IPMN-P, and we diagnosed them as IPNB. In contrast, both papillary and tubular structures were present in the remaining four tumors (17%), and three of these four tumors were duct-ectatic type without macroscopic mucin secretion. These features are common findings in ITN-P or ITPN-P, which are rare diseases[15,19-24]. These tubulopapillary tumors can be distinctly subcategorized in INihB based on their characteristic macroscopic and histological findings. Intraductal neoplasms with a tubular structure have been reported in the pancreatic area. Albores-Saavedra *et al*[19] reported that tumors with a tubular structure included: (1) glands resembling pyloric glands; (2) glands lined by cells with no cytoplasmic mucin and with mild nuclear atypia; and (3) glands lined by pink oncocytic cells. Recently, Yamaguchi *et al*[14] proposed the concept of ITPN-P and defined nine diagnostic criteria. Similarly, some authors have described intraductal lesions in which IPNB with formation of the tubular structure is regarded as intraductal tubular neoplasm of the bile duct (ITNB)[25,26]. In our four cases, we observed morphological similarity with ITN-P or ITPN-P. In particular, Case 1 consisted mainly of a tubular structure and some papillary patterns, and the neoplastic cells were markedly atypical. In addition, immunohistochemical results were MUC1(+) and MUC5AC(-), which were different from ITN-P. Our case 1 was considered as an ITPN-B subcategory. As discussed above, IPNB contained IPNB with a tubular structure, although small in number, and there might be cases with similar characteristics to ITN-P or ITPN-P.

We also examined Ki-67 and p53 immunoreactivity in the 24 cases of INihB. Ki-67 expression differed significantly between malignant and borderline/adenoma (22.2 ± 15.5 *vs* 7.5 ± 6.3, $P < 0.01$), but P53 was negative in all cases. Based on these data, Ki-67 LI correlates with the degree of malignancy in INihB. Shibahara *et al*[6] reported significantly high Ki-67 expression and poorer prognosis in the columnar type than in the cuboidal type. In this study, we also investigated the relationship between MUC1/MUC5AC immunostaining and malignant potential. Some studies have reported that the pancreatobiliary type IPMN-P, which is positive for MUC1, is highly malignant[8]. Other studies have suggested that MUC1 contributes significantly to tumor growth and metastasis, and that downregulation of MUC1 protein expression decreases the metastatic potential of pancreatic adenocarcinoma[27]. The association between MUC1 and malignant potential has also been suggested in cholangiocarcinoma[28]. Although we did not find a significant association between MUC5AC expression and the degree of malignancy or cell proliferation potential, there was a borderline association between the higher expression of MUC5AC and the higher Ki-67 LI in the malignant group. Some authors also have reported that MUC5AC is more strongly expressed in advanced tumors[17,28]. Thus, we suggest that expression of MUC1 and MUC5AC is related, MUC1 more strongly so than MUC5AC, to the degree of malignancy in INihB.

Nuclear expression of β-catenin was found in 8% of INihB (2/24), and MUC1 was also positive in these cases. β-catenin is a mediator in the canonical Wnt signal transduction pathway[29] and activation of the Wnt pathway is associated with high proliferation and dedifferentiation in human biliary tumors[30]. Nuclear accumulation of β-catenin was reported in 15% of intrahepatic cholangiocarcinomas (Sugimachi *et al*[31]); 25% of IPN-B, 20% of IPN-B associated with intrahepatic cholangiocarcinoma, and 0% of biliary intraepithelial neoplasms (Itatsu *et al*[32]); and 25% of IPN-B (Abraham *et al*[33]). The Wnt signaling pathway is frequently activated in biliary neoplasms[32]. We believe when dealing with INihB one should consider performing immunohistochemical staining for MUC1 and β-catenin, in addition to histomorphological examination, to evaluate malignant potential of the tumor.

In conclusion, we propose the concept of INihB that includes IPNB and IPNB with tubular structure subcategories, that is, ITNB and intraductal tubulopapillary neoplasm of the bile duct. IPNB with tubular structure is rare, and (1) is mostly duct-ectatic without macroscopic mucin hypersecretion; and (2) histologically, has both

papillary and tubular structures. In INihB, MUC1 expression correlates positively with the degree of malignancy and cell proliferation potential. MUC5AC expression also correlates with the degree of malignancy, although the relationship is less robust. Further pathological and molecular studies are necessary to clarify the characteristics of INihB.

COMMENTS

Background

The clinicopathological characteristics of intraductal neoplasm of the intrahepatic bile duct (INihB) remains unclear. In this article, the authors present the clinicopathological features of 24 cases of INihB.

Research frontiers

Some studies have reported that the pancreatobiliary-type intraductal papillary mucinous neoplasm (IPMN-P), which is positive for mucin (MUC)1 expression, is highly malignant, and other studies have suggested that MUC1 contributes significantly to tumor growth and metastasis, and that downregulation of MUC1 protein expression decreases the metastatic potential of pancreatic adenocarcinoma. The association between MUC1 and malignant potential has also been suggested in cholangiocarcinoma. Some authors have reported that MUC5AC is more strongly expressed by advanced tumors. In this study, the authors demonstrated that MUC1 and MUC5AC expression may be related to the malignant potential of INihB.

Innovations and breakthroughs

Recent reports have highlighted the relationship between MUC profile and malignancy potential. In particular, the authors investigated the relationship between MUC1/MUC5AC immunohistochemical staining and Ki-67 labeling index.

Applications

This study offers a better understanding of clinicopathological characteristics of INihB and a potential strategy to predict tumor behavior for better patient care.

Terminology

MUC1/MUC5AC are mucin proteins in the pancreatobiliary/gastric epithelium, respectively. It has been suggested that these proteins play an important role in tumor growth and metastasis in pancreatobiliary disease.

Peer review

Immunohistochemical analysis revealed that Ki-67 expression in the 24 INihBs was significantly high in the malignant group. MUC staining showed that MUC1 was not expressed in the borderline/adenoma group but was expressed only in malignant lesions, and the Ki-67 labeling index was significantly higher in the malignant group than in the borderline/adenoma group. These results may represent a mechanism of MUC protein in tumor growth, that is, malignant potential of the tumor.

REFERENCES

1 **Ohtsubo K**, Ohta H, Sakai J, Mouri H, Nakamura S, Ikeda T, Kifune K, Yoshikawa J, Harada K, Nakanuma Y, Watanabe H, Motoo Y, Okai T, Sawabu N. Mucin-producing biliary papillomatosis associated with gastrobiliary fistula. *J Gastroenterol* 1999; **34**: 141-144

2 **Lim JH**, Kim YI, Park CK. Intraductal mucosal-spreading mucin-producing peripheral cholangiocarcinoma of the liver. *Abdom Imaging* 2000; **25**: 89-92

3 **Sakamoto E**, Hayakawa N, Kamiya J, Kondo S, Nagino M, Kanai M, Miyachi M, Uesaka K, Nimura Y. Treatment strategy for mucin-producing intrahepatic cholangiocarcinoma: value of percutaneous transhepatic biliary drainage and cholangioscopy. *World J Surg* 1999; **23**: 1038-1043; discussion 1043-1044

4 **Kokubo T**, Itai Y, Ohtomo K, Itoh K, Kawauchi N, Minami M. Mucin-hypersecreting intrahepatic biliary neoplasms. *Radiology* 1988; **168**: 609-614

5 **Kim HJ**, Kim MH, Lee SK, Yoo KS, Park ET, Lim BC, Park HJ, Myung SJ, Seo DW, Min YI. Mucin-hypersecreting bile duct tumor characterized by a striking homology with an intraductal papillary mucinous tumor (IPMT) of the pancreas. *Endoscopy* 2000; **32**: 389-393

6 **Shibahara H**, Tamada S, Goto M, Oda K, Nagino M, Nagasaka T, Batra SK, Hollingsworth MA, Imai K, Nimura Y, Yonezawa S. Pathologic features of mucin-producing bile duct tumors: two histopathologic categories as counterparts of pancreatic intraductal papillary-mucinous neoplasms. *Am J Surg Pathol* 2004; **28**: 327-338

7 **Zen Y**, Sasaki M, Fujii T, Chen TC, Chen MF, Yeh TS, Jan YY, Huang SF, Nimura Y, Nakanuma Y. Different expression patterns of mucin core proteins and cytokeratins during intrahepatic cholangiocarcinogenesis from biliary intraepithelial neoplasia and intraductal papillary neoplasm of the bile duct--an immunohistochemical study of 110 cases of hepatolithiasis. *J Hepatol* 2006; **44**: 350-358

8 **Furukawa T**, Klöppel G, Volkan Adsay N, Albores-Saavedra J, Fukushima N, Horii A, Hruban RH, Kato Y, Klimstra DS, Longnecker DS, Lüttges J, Offerhaus GJ, Shimizu M, Sunamura M, Suriawinata A, Takaori K, Yonezawa S. Classification of types of intraductal papillary-mucinous neoplasm of the pancreas: a consensus study. *Virchows Arch* 2005; **447**: 794-799

9 **Adsay NV**, Adair CF, Heffess CS, Klimstra DS. Intraductal oncocytic papillary neoplasms of the pancreas. *Am J Surg Pathol* 1996; **20**: 980-994

10 **Isaji S**, Kawarada Y, Taoka H, Tabata M, Suzuki H, Yokoi H. Clinicopathological features and outcome of hepatic resection for intrahepatic cholangiocarcinoma in Japan. *J Hepatobiliary Pancreat Surg* 1999; **6**: 108-116

11 **Helpap B**. Malignant papillomatosis of the intrahepatic bile ducts. *Acta Hepatogastroenterol (Stuttg)* 1977; **24**: 419-425

12 **Kim YI**, Yu ES, Kim ST. Intraductal variant of peripheral cholangiocarcinoma of the liver with Clonorchis sinensis infection. *Cancer* 1989; **63**: 1562-1566

13 **Taguchi J**, Yasunaga M, Kojiro M, Arita T, Nakayama T, Simokobe T. Intrahepatic and extrahepatic biliary papillomatosis. *Arch Pathol Lab Med* 1993; **117**: 944-947

14 **Yamaguchi H**, Shimizu M, Ban S, Koyama I, Hatori T, Fujita I, Yamamoto M, Kawamura S, Kobayashi M, Ishida K, Morikawa T, Motoi F, Unno M, Kanno A, Satoh K, Shimosegawa T, Orikasa H, Watanabe T, Nishimura K, Ebihara Y, Koike N, Furukawa T. Intraductal tubulopapillary neoplasms of the pancreas distinct from pancreatic intraepithelial neoplasia and intraductal papillary mucinous neoplasms. *Am J Surg Pathol* 2009; **33**: 1164-1172

15 **Nakayama Y**, Inoue H, Hamada Y, Takeshita M, Iwasaki H, Maeshiro K, Iwanaga S, Tani H, Ryu S, Yasunami Y, Ikeda S. Intraductal tubular adenoma of the pancreas, pyloric gland type: a clinicopathologic and immunohistochemical study of 6 cases. *Am J Surg Pathol* 2005; **29**: 607-616

16 **Zen Y**, Fujii T, Itatsu K, Nakamura K, Minato H, Kasashima S, Kurumaya H, Katayanagi K, Kawashima A, Masuda S, Niwa H, Mitsui T, Asada Y, Miura S, Ohta T, Nakanuma Y. Biliary papillary tumors share pathological features with intraductal papillary mucinous neoplasm of the pancreas. *Hepatology* 2006; **44**: 1333-1343

17 **Zen Y**, Fujii T, Itatsu K, Nakamura K, Konishi F, Masuda S, Mitsui T, Asada Y, Miura S, Miyayama S, Uehara T, Katsuyama T, Ohta T, Minato H, Nakanuma Y. Biliary cystic tumors with bile duct communication: a cystic variant of intraductal papillary neoplasm of the bile duct. *Mod Pathol* 2006; **19**: 1243-1254

18 **Devaney K**, Goodman ZD, Ishak KG. Hepatobiliary cystadenoma and cystadenocarcinoma. A light microscopic and immunohistochemical study of 70 patients. *Am J Surg Pathol* 1994; **18**: 1078-1091

19 **Albores-Saavedra J**, Sheahan K, O'Riain C, Shukla D. Intraductal tubular adenoma, pyloric type, of the pancreas: ad-